



Bias-Adjusted Climate Change Projections over Singapore

10

Authors:

Aurel Florian Moise, Sandeep Sahany, Muhammad Eeqmal Hassim, Chen Chen, Xin Rong Chua, Venkatraman Prasanna, Gerald Lim, Pavan Harika Raavi, Jianjun Yu, Fei Luo



**METEOROLOGICAL
SERVICE
SINGAPORE**
Centre for Climate Research Singapore

© National Environment Agency (NEA) 2024

All rights reserved. No part of this publication may be reproduced, stored in a retrieval system, or transmitted in any form or by any means, electronic or mechanical, without the prior permission of the Centre for Climate Research Singapore.

10.1 Introduction

In this chapter, we present the climate change projections over Singapore using the 2km dynamically downscaled simulations that have been bias-adjusted to reduce systematic biases reported in Chapter 7 of this report. As discussed in Chapter 9, the 8km and 2km downscaled projections over Singapore were bias-adjusted using one of the advanced techniques recommended by ISIMIP3 (Lange, S. 2019).

Singapore's climate change projections are presented for annual and seasonal scales. For the seasons, 5 periods corresponding to Singapore's monsoon and intermonsoon transition seasons were selected: the northeast monsoon season, the southwest monsoon season and both the intermonsoons. The northeast monsoon season is further divided into the wet phase comprising the months of December and January, and the dry phase comprising the months February and March. The southwest monsoon season comprises the months of June through September, and the first and second intermonsoon periods occur in April-May and October-November respectively.

Specifically, we present changes in the mean state and extremes of some key variables under the three SSP scenarios for the mid- and end-century 20-year periods:

Changes in rainfall: For mean rainfall, we present changes in the annual and seasonal mean rainfall. For rainfall extremes, we present changes in the maximum daily rainfall (RX1day), maximum 5-day rainfall (RX5day), the 95th and 99.9th percentiles in each season and for the annual timescale. Changes are only shown for the end-century period under the SSP5-8.5 scenario.

Changes in temperature: For mean temperature, we present changes in the annual and seasonal mean temperature, and for temperature extremes we present changes in the daily maximum temperature, daily minimum temperature, annual maximum temperature, annual minimum temperature, the 95th and 99.9th percentiles.

Changes in heat stress: For heat stress index, we present changes in the wet bulb globe

temperature (WBGT) for annual and various seasons.

Changes in relative humidity: For relative humidity, we present changes in the 2m relative humidity for annual and various seasons.

Changes in near- surface winds: For winds, we present changes in the 10m wind speed for annual and various seasons. For wind gusts we present changes in wind gusts during the mid- and end-century for SSP5-8.5.

Finally, we also compare the similarities and differences in the projected rainfall and temperature changes over Singapore from the 8 km bias-adjusted data with the 2 km bias-adjusted data.

In the figures where we show projected changes for the mid- and end-century for the 3 SSPs, we document the changes for each of the periods by referring to the changes shown by the multi-model mean (thin line) in the 3 SSPs followed by the range (lowest projected change to highest projected change) within each SSP shown in brackets.

10.2 Changes in Mean Rainfall

Figure 10.1 shows the projected changes in the mean rainfall, area-averaged over Singapore, under the 3 SSP scenarios for the entire year (annual) and different seasonal periods as presented in Section 10.1.

10.2.1 Annual Rainfall

Overall, across all scenarios, the multi-model average in annual mean rainfall is projected to increase or remain the same both in the mid- and end-century. However, the magnitude of change varies going from mid-century to end-century between the scenarios (Table 10.1, Figure 10.1): an increase is projected in SSP1-2.6 (5% to 11%), almost no change is projected for SSP2-4.5 (i.e. remaining at 5%), and a decrease is projected in SSP5-8.5 (from 10% to 0%). The large drop in projected mean change in SSP5-8.5 from the mid-to-end century is largely due to the increased spread between the models (i.e. lack of model

consensus in the sign of change by the end-century). The differences seen between the scenarios indicate that the local change in annual mean rainfall change does not necessarily scale

with global warming, unlike the global average as reported in IPCC AR6. There can be significant differences on regional and local scales, as seen for Singapore.

Table 10.1: Projected changes in annual mean rainfall (percent change)

Scenario	Mid-Century Annual Rainfall Change (%)		End-Century Annual Rainfall Change (%)	
	Mean	Range	Mean	Range
SSP1-2.6	5	-2 to 8	11	0 to 24
SSP2-4.5	5	-2 to 12	5	-6 to 12
SSP5-8.5	10	-5 to 19	0	-12 to 17

While there is a similar annual mean rainfall by 2100, we observe that the year-to-year variation has increased over time, particularly towards the second half of the 21st century (not shown). The change in variability is most likely related to the change in ENSO behavior in the future. New evidence suggests that ENSO variability will likely increase in the future i.e., more extreme El Ninos and La Niñas (Cai et al., 2014, 2021).

Although the annual mean rainfall is projected to increase/remain same both in the mid- and end-

century across all scenarios, the seasonal mean changes differ across seasons. Based on the multi-model mean changes in SSP5-8.5, there are increases in wet months (e.g. DJ) and decreases in dry months (e.g. FM, JJAS) at the end of the century. This increased contrast between seasons was noted in the 2nd National Climate Change Study (V2), and might be linked to the narrowing of the ITCZ projected by global models (e.g. Byrne and Schneider., 2016). We discuss these changes in detail below.

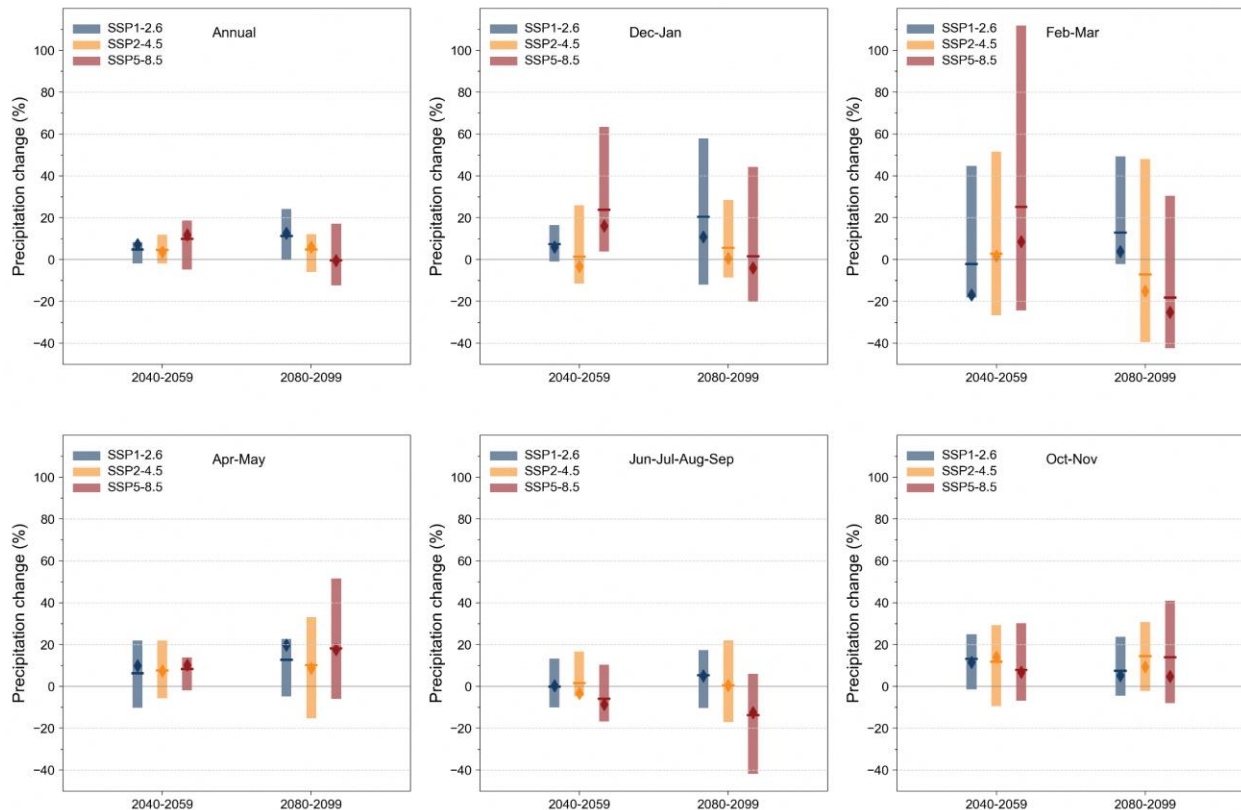


Figure 10.1: Percentage change of rainfall total (pr) in the Annual, December–January, February–March, April–May, June–July–August–September, and October–November for mid- (2040–2059) and end-century (2080–2099) periods from the 5 bias-

adjusted downscaled GCMs (2 km) over Singapore relative to the baseline (1995–2014). The line and diamond represent the mean and median using the 5 models, respectively. For readability, the values are available in Tables 10.1-10.6.

10.2.2 December-January (DJ) rainfall (wet phase of NE monsoon)

The projected changes in DJ rainfall follow a similar pattern to the change in mean annual rainfall. Overall, DJ rainfall is projected to increase by the end of the century across all scenarios. However, the magnitude of change differs between the scenarios. While the average DJ rainfall is projected to increase even more under SSP1-2.6 (from 7% in mid-century to 20% in end-

century), the projected changes are considerably smaller under SSP2-4.5 and especially in SSP5-8.5 (24% in mid-century to only 2% in end-century). This suggests that local DJ rainfall changes over Singapore do not scale with the level of global warming. In chapter 8, we noted a slight increase in the frequency of NE monsoon surges from November to February (NDJF), with small changes in the magnitude of rainfall during surge days. It is possible that the changes would be different in other scenarios, or even in DJ as opposed to NDJF.

Table 10.2: Projected Changes in DJ Mean Rainfall (percent change)

DJ	Mid-Century Dec-Jan Rainfall Change (%)		End-Century Dec-Jan Rainfall Change(%)	
	Mean	Range	Mean	Range
SSP1-2.6	7	-1 to 16	20	-12 to 58
SSP2-4.5	1	-12 to 26	6	-9 to 28
SSP5-8.5	24	4 to 63	2	-20 to 44

However, there is a general agreement among the model projections for the wet phase of the NE monsoon season to become slightly wetter, consistent with the finding in the 2nd National Climate Change Study (V2). This could be due to a multitude of factors such as changing characteristics of Borneo Vortices, which could become less frequent but bring more rainfall (Liang et al., 2021), an increase in MJO-related rainfall from the second half of the 21st century

(Bui et al., 2023) and/or the occurrence of more El Ninos (Cai et al., 2021; Geng et al., 2022). Note that while El Nino is known to reduce rainfall across many parts of the region during NE monsoon season, historical climatological records show that local December rainfall for Singapore actually increases during El Nino events and decreases during La Nina events, compared to ENSO-neutral conditions (no El Nino or La Nina in the Pacific).

10.2.3 February-March (FM) rainfall (dry phase of NE monsoon)

The projections for February-March mean rainfall indicate a drying tendency for the 2nd half of the 21st century under the moderate (SSP2-4.5) and high warming (SSP5-8.5) scenarios. This is in contrast to a projected increase under the low warming (SSP1-2.6) scenario (-2% mid-century to 13% end-century). The reasons for the difference in the sign of change between the scenarios by the end of the century are unclear at this stage but could be related to the differences in the timing, magnitude and regional impacts of decadal-scale variability between the scenarios (Johnson et al., 2020). In addition, the high mean change value for the mid-century under the SSP5-8.5 scenarios

(25%) is positively skewed by an outlier model (c.f. mid-century range is -24 to 112 %). Likewise, the projected mid-century mean change under SSP1-2.6 is also positively skewed by an outlier model (c.f. the separation between the median diamond and mean thin line markers, Figure 10.1).

Nonetheless, the signs of the end-century projected changes under SSP2-4.5 and SSP5-8.5 reported here are consistent with the end-century changes projected in V2 for the same months. Under the RCP8.5 scenario, six out of nine models projected a statistically significant decreasing signal of more than 30% change in mean February rainfall towards the end of the century (Figure 5.23, Marzin et al. 2015). This suggests that the projected drying trend in the

drier phase of the NE monsoon is likely to be robust and could be associated with stronger cross-equatorial flow in the future (Liang et al., 2022). Cross-equatorial northerly surges are a feature during the drier phase of the NE monsoon. These tend to shift the rainband south of the equator and into the Java Sea, thereby reducing rainfall over Singapore.

Overall, the findings here suggest that NE monsoon could experience a much greater intra-seasonal contrast in the future by the end of the century with the wet phase of the NE monsoon projected to become slightly wetter and the drier phase NE monsoon likely to become drier.

Table 10.3: Projected Changes in FM Mean Rainfall (percent change)

FM	Mid-Century Feb-Mar Rainfall Change (%)		End-Century Feb-Mar Rainfall Change (%)	
	Mean	Range	Mean	Range
SSP1-2.6	-2	-18 to 45	13	-2 to 49
SSP2-4.5	3	-27 to 52	-7	-39 to 48
SSP5-8.5	25	-24 to 112	-18	-43 to 30

10.2.4 April-May (AM) and October-November (ON) rainfall (first and second intermonsoon periods)

The first (AM) and second (ON) intermonsoon periods both exhibit very similar positive changes both in the mid-century and end-century. Overall, both intermonsoon periods show increased mean rainfall by the end of the century across the scenarios, although there is a slight reduction in the positive change of ON mean rainfall under SSP1-2.6 (from 13% to 8%). Under SSP1-2.6, most of the warming in global mean and local Singapore temperatures takes place by mid-century. As such, there is not expected to be much additional influence of warming on rainfall from

mid-century to end-century. As such, the reduction in the magnitude of the positive change from mid-century to end-century in ON rainfall is more likely due to decadal variability. This is also most likely the case for AM mean rainfall.

In contrast, the magnitude of change under SSP2-4.5 and SSP5-8.5 for AM and ON mean rainfall both increase by the end of the century, and are likely to be governed more by the climate change signal. Both the scenarios show increases of mean rainfall with warming from mid- to end-century, albeit at different rates (e.g. from 12% to 14% under SSP2-4.5, and from 8% to 14% under SSP5-8.5 for ON rainfall, see Table 10.5).

Table 10.4: Projected Changes in AM Mean Rainfall (percent change)

AM	Mid-Century Apr-May Rainfall Change (%)		End-Century Apr-May Rainfall Change (%)	
	Mean	Range	Mean	Range
SSP1-2.6	6	-10 to 22	13	-5 to 23
SSP2-4.5	8	-6 to 22	10	-15 to 33
SSP5-8.5	8	-2 to 14	18	-6 to 52

Table 10.5: Projected Changes in ON Mean Rainfall (percent change)

ON	Mid-Century Oct-Nov Rainfall Change (%)		End-Century Oct-Nov Rainfall Change (%)	
	Mean	Range	Mean	Range
SSP1-2.6	13	-1 to 25	8	-4 to 24
SSP2-4.5	12	-9 to 29	14	-2 to 31
SSP5-8.5	8	-7 to 30	14	-8 to 41

10.2.5 June-September (JJAS) rainfall (SW monsoon)

As in FM rainfall, the SW monsoon season only shows an increase in mean JJAS rainfall from mid- to end-century under the SSP1-2.6 scenario, while the other scenarios show slight change

(SSP2-4.5) or a reduction in rainfall (SSP5-8.5). The behavior under SSP1-2.6 is likely again to be associated with decadal variability while the response under SSPs 2-4.5 and 5-8.5 are more likely related to the warming climate, with JJAS rainfall potentially reducing by an average of 14% by 2100.

The mechanism for this drying trend could be related to how SST warming patterns in the tropical Pacific might change in the future to become more El Niño-like. Such changes are known to greatly affect the southwestern Maritime Continent region (Ghosh & Shepherd, 2023).

Recent work by CCRS suggests that seasonal rainfall totals are likely to fluctuate even more in the future due to the stronger relationship that ENSO exerts over rainfall in the Western Maritime Continent region during the Southwest Monsoon season (Chen et al., 2023). For the influence of ENSO, we also showed in Chapter 8 section 8.4.3

that GCMs and RCMs both suggest that ENSO-induced negative teleconnection area over the equatorial MC is enlarged under warming.

An even drier JJAS season increases the risk of peatland and forest fires and thus transboundary haze for this highly vulnerable region. The drying signal is considered robust since it further supports the findings from V2 (in which four of nine models showed statistically significant decreases in mean rainfall at the end of the 21st century under the RCP 8.5 scenario, see Figure 5.22b, Marzin et al., 2015).

Overall, we find that the projected mean rainfall change varies in sign and magnitude across the seasons for both mid- and end-century periods and for all scenarios. The largest range in probable outcomes is shown for February-March (due to an outlier).

Table 10.6: Projected Changes in JJAS Mean Rainfall (percent change)

JJAS	Mid-Century Jun-Sep Rainfall Change (%)		End-Century Jun-Sep Rainfall Change (%)	
	Mean	Range	Mean	Range
SSP1-2.6	0	-10 to 13	5	-10 to 17
SSP2-4.5	2	-5 to 17	0	-17 to 22
SSP5-8.5	-6	-17 to 10	-14	-42 to 6

The end-century changes under SSP1-2.6 are more likely to be related to decadal variability while the projected changes under SSP2-4.5 and

especially SSP5-8.5 are likely a response to the increased warming brought by increasing greenhouse gas emissions.

10.3 Changes in Rainfall Extremes

Extreme rainfall – as represented by the average maximum 1-day and 5-day totals on annual and seasonal time scales – is expected to increase considerably by the end of the 21st century. In Chapter 8 Section 8.3.3, we showed that extreme rainfall changes across Southeast Asia. Here in this section of Chapter 10, we focus on Singapore to address changes in the rainfall extremes. The increases in both extreme rainfall metrics occur for all seasons and across all of Singapore except for February and March, in which a reduction in the average intensity of RX1day and RX5day is projected over the northern, central and southern parts of Singapore (Figure 10.2 and Figure 10.3). Interestingly, increases in average RX1day and RX5day rainfall (10-45%) are still projected for the

easternmost and westernmost areas of Singapore during the dry phase of the NE monsoon.

The areas with the highest projected percentage increases vary with season. Overall, the largest values occur during the intermonsoon periods. Specifically, the biggest changes (40-50% relative to the 1995-2014 baseline) are seen over the western and central areas during the first inter monsoon period (April-May), while these are concentrated to the far east of Singapore during the second intermonsoon (October-November).

In contrast, the wet NE monsoon (December-January) and the SW monsoon periods show smaller projected increases across Singapore. There is a southwest-to-northeast gradient in the pattern of intensity change during the SW

monsoon (June-September) with relatively higher percentage increases projected in mean RX1day and RX5day for the northeastern areas and lower in the southwest portions of the country. The spatial pattern of percentage increases is more heterogeneous during the wet phase of the NE monsoon.

Notably, the spatial pattern of both RX1day and RX5day average intensity changes are very similar. This suggests that RX5day extremes are dominated by the extreme rainfall amounts on daily time scales. The overall increase in both average RX1day and RX5day intensities in all seasons except for the NE monsoon dry period is

consistent with the expectation that rainfall (wet) extremes will become more severe in a warming world (Seneviratne et al., 2021).

The increases in mean RX1day and RX5day imply that there are changes to the future characteristics of extreme precipitation events typical for the season. For the two intermonsoon periods, daily rainfall is often dominated by the frequent diurnal occurrence of afternoon convective thunderstorms. The strong increase in mean RX1Day rainfall suggests that future convective thunderstorms are either more intense and/or lasting longer, on average, than those in the current climate.

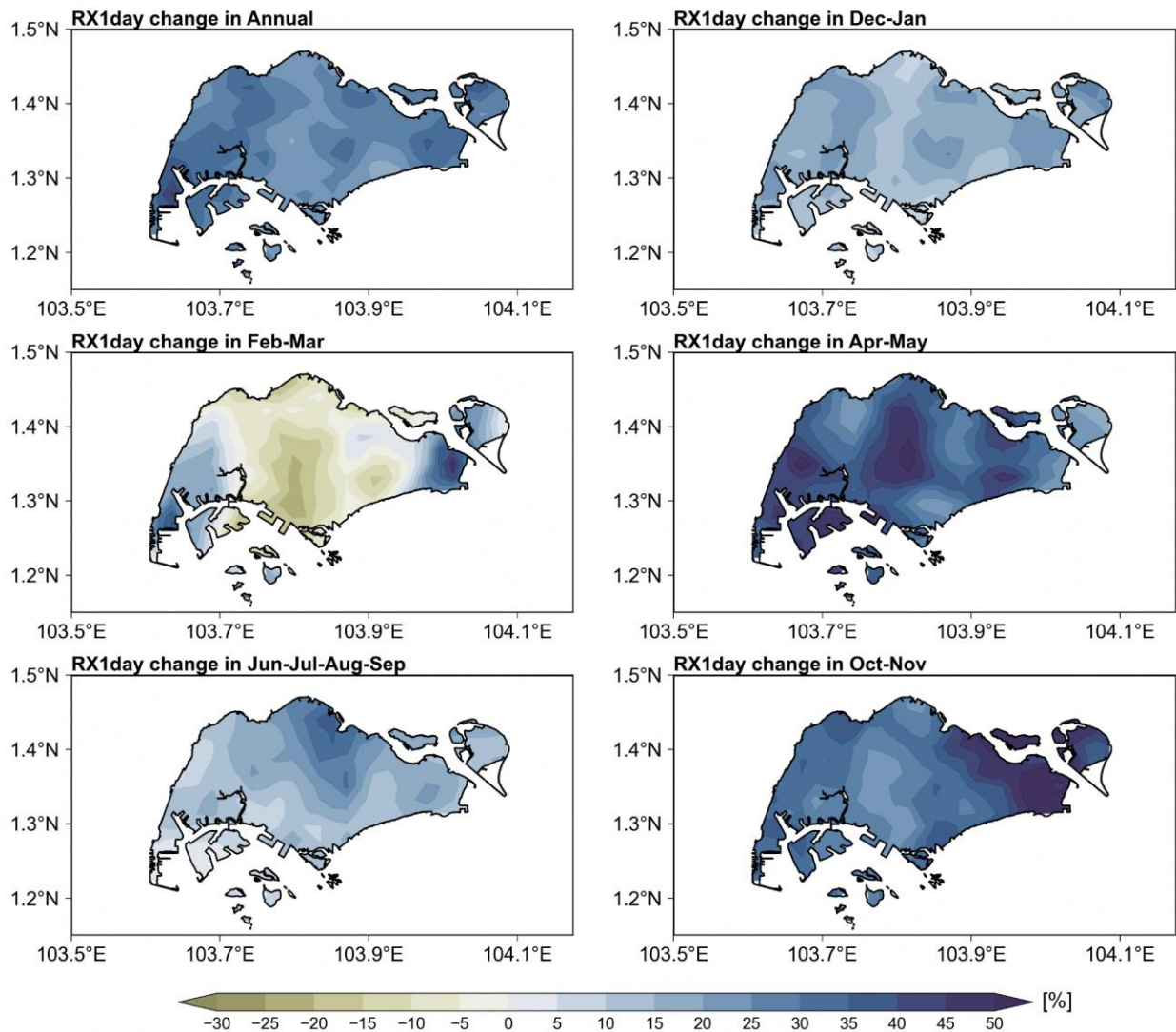


Figure 10.2: Ensemble mean (5 bias-adjusted 2km downscaled GCMs) percentage change of maximum 1-day (Rx1day) precipitation in annual, December–January, February–March, April–May, June–July–August–September, and October–

November months during end-century (2080–2099) period relative to the baseline (1995–2014) over Singapore under the SSP5-8.5 scenario.

For the NE monsoon wet phase, extreme daily rainfall values in the historical observations are likely caused by strong monsoon surges. The projected increases in mean RX1day and RX5day for the two intermonsoons and the wet NE

monsoon phase suggest that rainfall associated with strong monsoon surges have become more severe (i.e. more total rainfall associated with them).

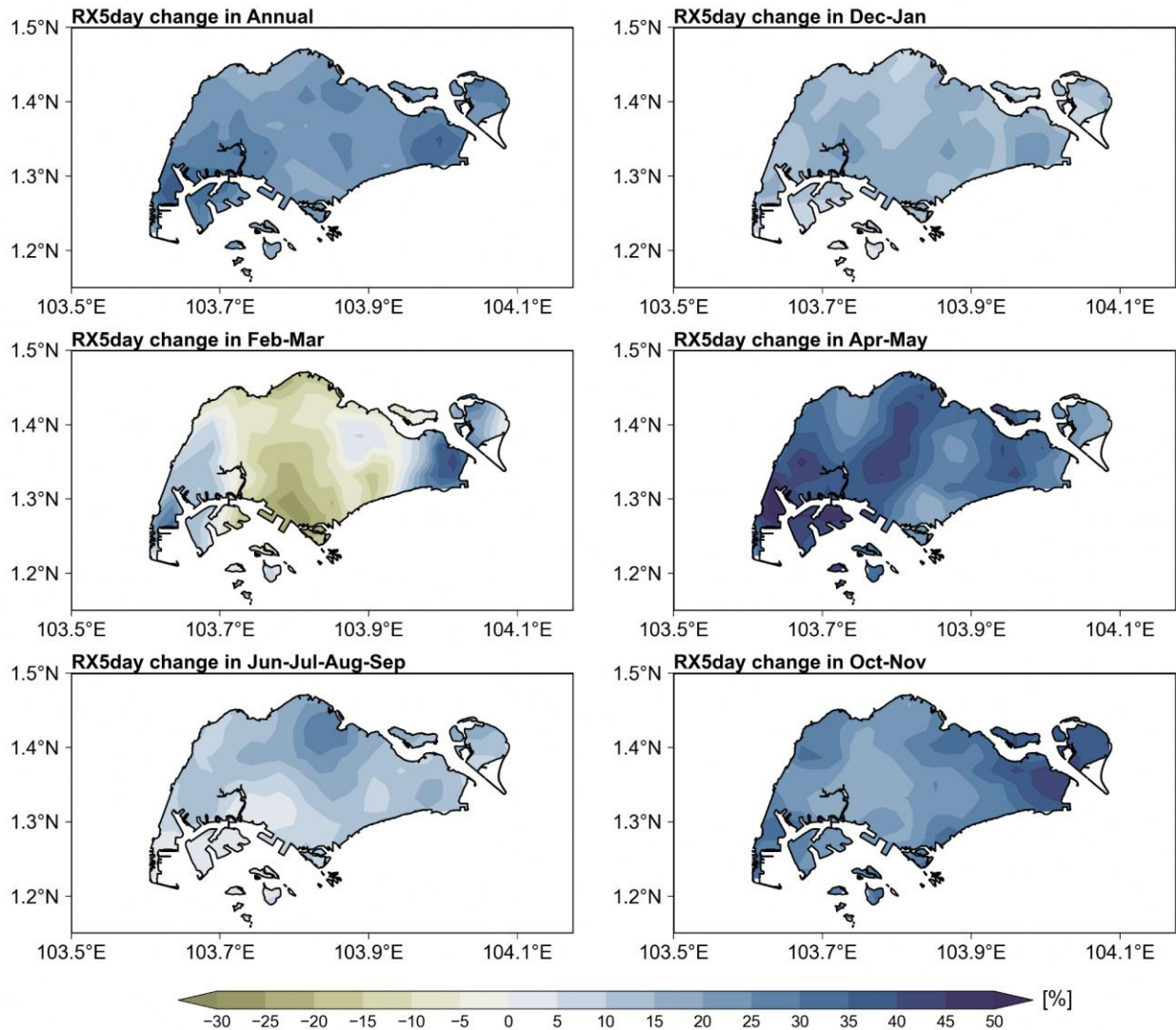


Figure 10.3: Ensemble mean (5 bias-adjusted 2km downscaled GCMs) percentage change of annual maximum 5-day (Rx5day) precipitation in annual, December–January, February–March, April–May, June–July–August–September, and October–November months during end-century (2080–2099) period relative to the baseline (1995–2014) over Singapore under the SSP5-8.5 scenario.

Note that, as we showed in Chapter 8 Section 8.3, Singapore is in between regions of increase and decrease for both mean rainfall and extremes in all seasons, so it is likely that a small shift in either direction could change the sign of the projected change over Singapore. Therefore, we need to be

careful to interpret the detailed spatial changes across Singapore.

Precipitation extremes over the entire Singapore are measured using the 95th and 99.9th percentiles of daily rainfall distributions. Figure

10.4 shows the percentage changes in the extreme rainfall percentiles (95th and 99.9th) in the mid-century and end century under SSP5-8.5 scenario relative to historical period at annual and seasonal time scales. As seen in the figure, the extreme rainfall is projected to increase but vary

at annual and seasonal time scales both in mid and end century.

At annual time scales (Table 10.7), both the multi-model mean 95th and 99.9th percentile of daily rainfall experience larger rises in the mid-century compared to the end-century period.

Table 10.7: Projected percentage changes in extreme daily rainfall percentiles (ANN)

ANN	Percentage change in annual extreme Rainfall (SSP5-8.5)			
	95th Percentile		99.9th Percentile	
	Mean	Range	Mean	Range
Mid century	15.6	0.6 to 24.2	39.4	9.3 to 64.6
End century	11.9	-0.3 to 21	26.4	12.7 to 43

During the northeast monsoon wet season (DJ; Table 10.8), 95th percentile rainfall in the mid century has a larger range compared to the end-century values; both the 95th and 99.9th percentile rainfall show reductions from their mid-century values to smaller increases in the end-century.

For the northeast monsoon dry season (FM; Table 10.9 and Fig. 10.4), the 95th and 99.9th percentile rainfall in the mid century has the largest range among the models. Towards the end of the century, both the 95th and 99.9th percentiles reduced from their mid-century values.

Table 10.8: Projected changes in extreme daily rainfall percentiles (DJ)

DJ	Percentage change in Dec-Jan extreme Rainfall (SSP5-8.5)			
	95th Percentile		99.9th Percentile	
	Mean	Range	Mean	Range
Mid century	31.5	6 to 92.8	50.6	28.6 to 88.2
End century	11.7	-17.1 to 50.9	36.2	26.3 to 42.9

Table 10.9: Projected changes in extreme daily rainfall percentiles (FM)

FM	Percentage change in Feb-Mar extreme Rainfall (SSP5-8.5)			
	95th Percentile		99.9th Percentile	
	Mean	Range	Mean	Range
Mid century	31.8	-19.6 to 118.5	47.6	-3.8 to 144.2
End century	-11.1	-40 to 29.5	20.2	-10.6 to 50.9

In contrast to the northeast monsoon season, the multi-model mean precipitation extremes (95th and 99.9th) over the first intermonsoon (AM; Table 10.10, and second intermonsoon (ON; Table 10.12) season rise towards the end of the century.

The southwest monsoon season shows a small decrease in the multi-model mean 95th percentile but 50 % increase (from 19.4 to 29.3 % change) for the 99.9th percentile.

Table 10.10: Projected changes in extreme daily rainfall percentiles (AM)

AM	Percentage change in Apr-May extreme Rainfall (SSP5-8.5)			
	95th Percentile		99.9th Percentile	
	Mean	Range	Mean	Range
Mid century	12.2	3.3 to 19	25.7	10 to 41.9

End century	27.4	5.3 to 58.3	53.4	21.6 to 91.6
-------------	------	-------------	------	--------------

Table 10.11: Projected changes in extreme daily rainfall percentiles (ON)

ON	Percentage change in Oct-Nov extreme Rainfall (SSP5-8.5)			
	95th Percentile		99.9th Percentile	
	Mean	Range	Mean	Range
Mid century	13.5	-0.3 to 27.9	23.7	9.2 to 38.7
End century	26.0	8.5 to 48.3	46.8	31.3 to 75.0

Table 10.12: Projected changes in extreme daily rainfall percentiles (JJAS)

JJAS	Percentage change in Jun-Sep extreme Rainfall (SSP5-8.5)			
	95th Percentile		99.9th Percentile	
	Mean	Range	Mean	Range
Mid century	0.8	-10.9 to 14.1	19.4	10.9 to 29.6
End century	0.2	-25.7 to 16.5	29.3	18.9 to 36.9

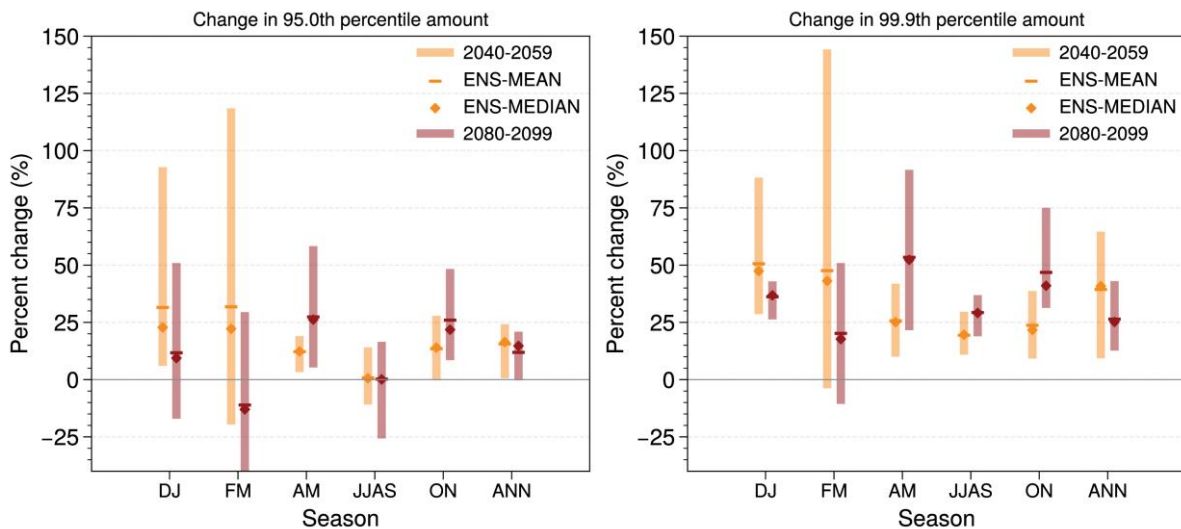


Figure 10.4: Percentage changes in 95th and 99.9th daily rainfall percentile amounts for annual and various seasons from the 2-km bias-adjusted SINGV-RCM simulations during the mid- (orange) and end-century (red) for SSP5-8.5. The line and diamond represent the mean and median using the 5 models, respectively. Rainfall percentiles are based on all days, pooled over all Singapore grid points; each percentile uses the nearest corresponding daily rainfall value. For readability, the values have been provided in Table 10.7-10.12.

The drought conditions over a region are measured using the maximum number of consecutive dry days (dry spell length). Figure 10.5 shows the annual maximum dry spell length (i.e. consecutive dry days) over Singapore in historical (1995-2014) and future (i.e. mid-century (2040-59) and end century (2080-99) under three SSP scenarios) time periods. As seen in Figure

10.5 and Table 10.13, the multi-model mean dry spell length in SSP5-8.5 increases with warming in the mid-century (~21 days) and end century (~23 days) relative to historical periods (Table 10.13). The increased dry spell length in a future warmer climate could put more stress on the water resources and energy consumption of Singapore.

Table 10.13: Historical and projected annual maximum dry spell length

	Mean dry spell length (days)	Dry spell length range (days)
Historical	21.1	18.5 to 22.3

Future	Mid-Century		End-Century	
	Mean	Range	Mean	Range
SSP1-2.6	22.3	21 to 25	21	20.3 to 22
SSP2-4.5	21.7	18.5 to 24.2	23	20.8 to 25.7
SSP5-8.5	21.8	18.7 to 24.8	23.3	18.7 to 25.7

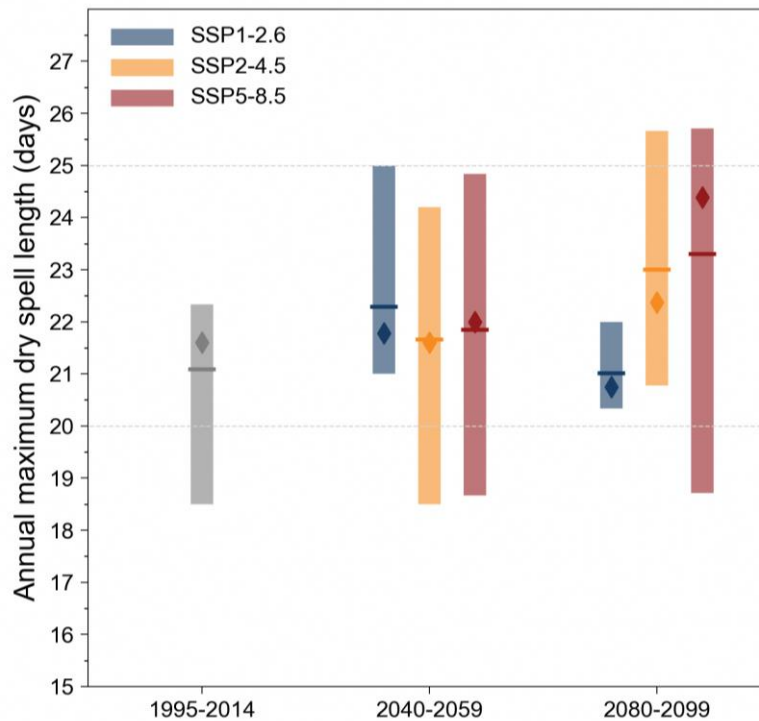


Figure 10.5: Historical and future annual maximum dry spell length for mid- (2040–2059) and end-century (2080–2099) periods from the 5 bias-adjusted downscaled GCMs (2 km) over Singapore relative to the baseline (1995–2014). The line and diamond represent the mean and median using the 5 models, respectively. For readability, the values are available in Tables 10.13.

Figure 10.6 shows the annual number of dry spells for more than 5 consecutive dry days over Singapore in historical and future (i.e. mid-century and end century under three SSP scenarios) time periods. As seen in Figure 10.6 and Table 10.14, the multi-model mean annual dry spell numbers under the SSP5-8.5 scenario are projected to increase in mid-century (~0.4) and end century

(~0.7) compared to historical periods. On average, Singapore could experience a dry spell from once every ten months (1/1.2 multiplied by 12) to once every sixty months (1/0.2 multiplied by 12). The increased number of dry spells would be expected to increase the frequency of droughts over Singapore.

Table 10.14: Historical and projected changes in annual dry spell (length >= 15 days) numbers

	Mean dry Spell number (count)		Dry spell number range (count)	
	Mean	Range	Mean	Range
Historical	0.2		0.1 to 0.3	
Future	Mid-Century		End-Century	
	Mean	Range	Mean	Range
SSP1-2.6	0.3	0.2 to 0.7	0.3	0.2 to 0.5
SSP2-4.5	0.3	0.25 to 0.35	0.6	0.45 to 0.75
SSP5-8.5	0.4	0.2 to 0.6	0.7	0.4 to 1.2

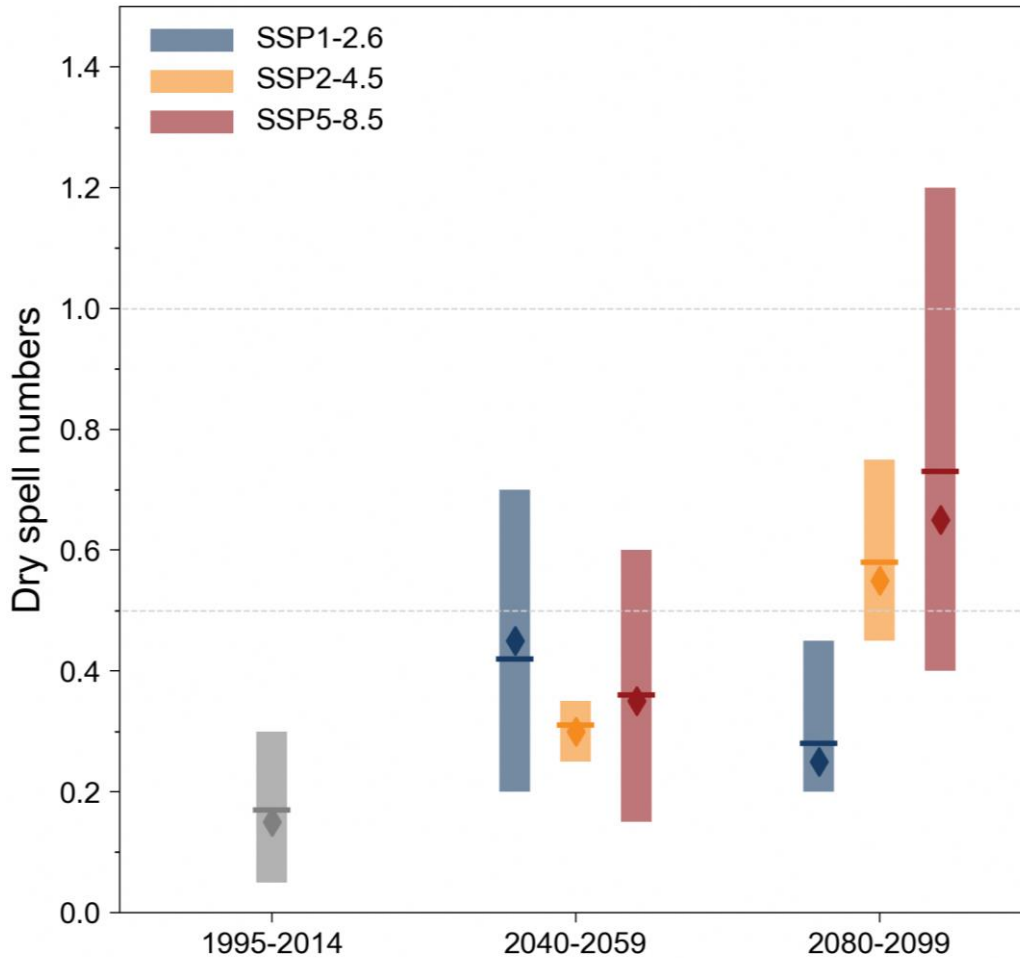


Figure 10.6: Historical and future annual number of dry spells for mid- (2040–2059) and end-century (2080–2099) periods from the 5 bias-adjusted downscaled GCMs (2 km) over Singapore relative to the baseline (1995–2014). The line and diamond represent the mean and median using the 5 models, respectively. For readability, the values are available in Tables 10.14.

10.4 Changes in Mean Temperature

Figure 10.7 shows the projected changes in the mean temperatures over Singapore under 3 SSP scenarios at different timescales in the mid- (2040-2059) and end-century (2080-2099) relative to the historical (1995-2014). As seen in Figure 10.7, the mean temperatures are projected to increase under the three scenarios both in mid- and end-century at annual (Table 10.15) and seasonal time scales (Table 10.16-10.20). The southwest monsoon (JJAS) and the second intermonsoon period (ON) seasons noted the biggest rises in surface temperatures at the end of

the century, each by 3.9°C and 4.0°C, respectively. At the end of the century, the annual mean surface temperatures are projected to increase by 1.1°C, 2.0°C, 3.8°C under the SSP1-2.6, SSP2-4.5, and SSP5-8.5 respectively. Also note that, for each scenario and time period, the changes for each season are very similar to one another.

From these projections we can infer that under the low-emission scenario of SSP1-2.6, temperature over Singapore will generally rise further by at least 1 degree during both mid- and end-century.

Table 10.15: Projected changes in annual mean near-surface air temperature

ANN	Mid-Century (°C)		End-Century (°C)	
	Mean	Range	Mean	Range
SSP1-2.6	1.0	0.6 to 1.3	1.1	0.6 to 1.6
SSP2-4.5	1.2	0.8 to 1.7	2.0	1.4 to 2.8
SSP5-8.5	1.6	0.9 to 2.2	3.8	2.8 to 5.0

Table 10.16: Projected changes in DJ mean near-surface air temperature

DJ	Mid-Century (°C)		End-Century (°C)	
	Mean	Range	Mean	Range
SSP1-2.6	0.9	0.6 to 1.2	1.0	0.5 to 1.6
SSP2-4.5	1.1	0.7 to 1.6	1.9	1.3 to 2.7
SSP5-8.5	1.5	0.9 to 2.1	3.7	2.6 to 4.7

Table 10.17: Projected changes in FM mean near-surface air temperature

FM	Mid-Century (°C)		End-Century (°C)	
	Mean	Range	Mean	Range
SSP1-2.6	1.0	0.5 to 1.4	1.1	0.5 to 1.7
SSP2-4.5	1.2	0.7 to 1.7	2.0	1.2 to 2.8
SSP5-8.5	1.5	0.8 to 2.1	3.7	2.5 to 5.1

Table 10.18: Projected changes in AM mean near-surface air temperature

AM	Mid-Century (°C)		End-Century (°C)	
	Mean	Range	Mean	Range
SSP1-2.6	1.0	0.6 to 1.3	1.2	0.6 to 1.7
SSP2-4.5	1.3	0.7 to 1.7	2.1	1.3 to 2.8
SSP5-8.5	1.5	0.8 to 2.1	3.8	2.6 to 5.0

Table 10.19: Projected changes in ON mean near-surface air temperature

ON	Mid-Century (°C)		End-Century (°C)	
	Mean	Range	Mean	Range
SSP1-2.6	0.9	0.7 to 1.3	1.1	0.6 to 1.6
SSP2-4.5	1.2	0.9 to 1.7	2.0	1.4 to 2.8
SSP5-8.5	1.6	1.1 to 2.2	4.0	2.9 to 5.1

Table 10.20: Projected changes in JJAS mean near-surface air temperature

JJAS	Mid-Century (°C)		End-Century (°C)	
	Mean	Range	Mean	Range
SSP1-2.6	1.0	0.7 to 1.3	1.1	0.6 to 1.6
SSP2-4.5	1.2	0.8 to 1.7	2.1	1.5 to 2.8
SSP5-8.5	1.6	0.9 to 2.2	3.9	3.1 to 5.0

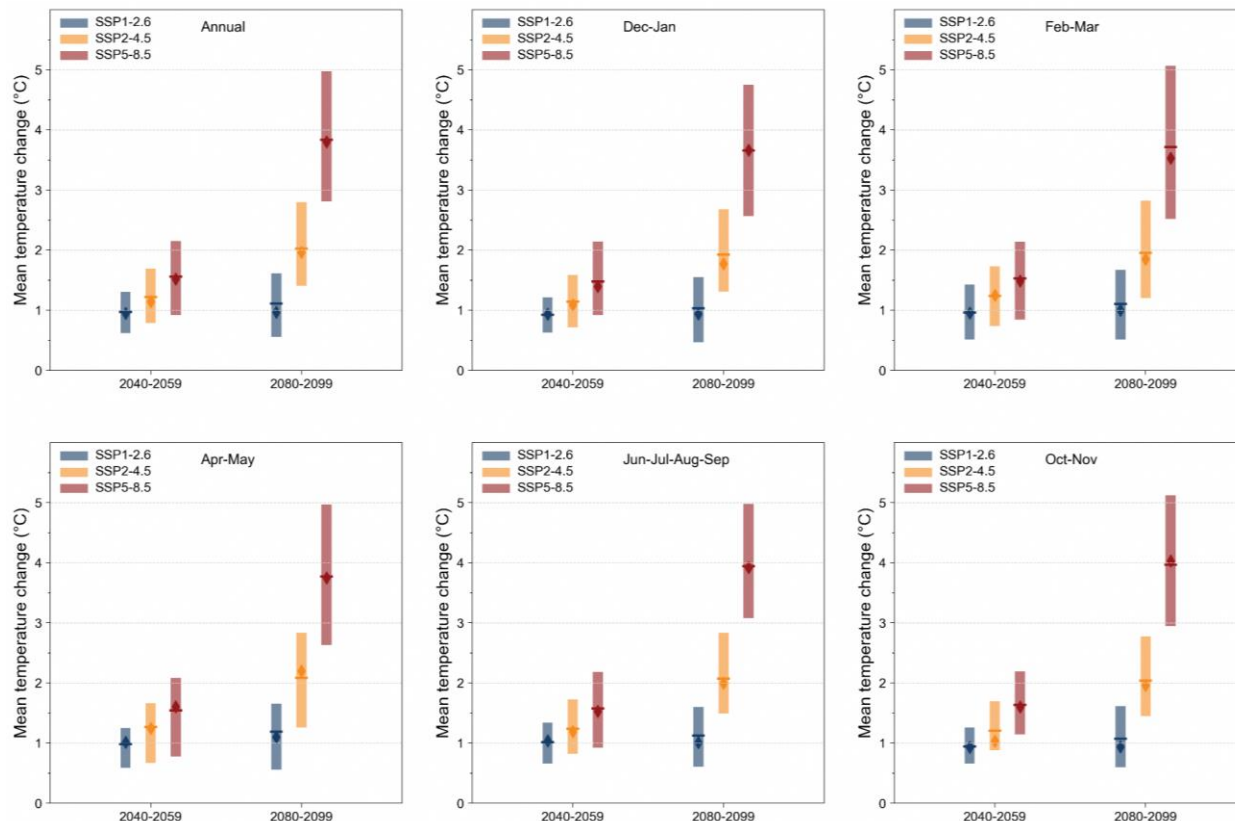


Figure 10.7: Change in mean daily near-surface air temperature in annual, December–January, February–March, April–May, June–July–August–September, and October–November during mid- (2040–2059) and end-century (2080–2099) periods from the 5 bias-adjusted downscaled GCMs (2 km) over Singapore relative to the baseline (1995–2014). The line and thin diamond represent the mean and median from the 5 models, respectively. For readability, the values are available in Tables 10.15–10.20.

10.5 Changes in Temperature Extremes

Temperature extremes of a region can be determined using the mean daily maximum and mean daily minimum temperatures. Figure 10.8 shows the projected changes in the extreme temperatures across Singapore under the three SSPs in the mid-century (2040–2059) and the end-

century (2080–2099). As seen in Figure 10.8, Singapore’s daily maximum (Table 10.21) and daily minimum temperatures (10.22) are projected to increase under the three scenarios both in the mid- and end-century. In the mid century, the daily maximum and daily minimum temperatures can increase by 1.6°C under the SSP5-8.5 scenario. Towards the end of the century, the daily maximum and daily minimum temperatures can increase by 4.0°C under the SSP5-8.5 scenario.

Table 10.21: Projected changes in annual mean daily maximum temperature

ANN	Mid-Century (°C)		End-Century (°C)	
	Mean	Range	Mean	Range
SSP1-2.6	1.0	0.6 to 1.4	1.1	0.5 to 1.7
SSP2-4.5	1.2	0.8 to 1.8	2.1	1.4 to 3.0
SSP5-8.5	1.6	0.9 to 2.2	4.0	2.9 to 5.3

Table 10.22: Projected changes in annual mean daily minimum temperature

ANN	Mid-Century (°C)		End-Century (°C)	
	Mean	Range	Mean	Range
SSP1-2.6	1.0	0.6 to 1.4	1.1	0.5 to 1.7
SSP2-4.5	1.2	0.8 to 1.8	2.1	1.4 to 3.0
SSP5-8.5	1.6	0.9 to 2.2	4.0	2.9 to 5.3

SSP1-2.6	1.0	0.6 to 1.3	1.1	0.6 to 1.6
SSP2-4.5	1.2	0.8 to 1.7	2.1	1.5 to 2.8
SSP5-8.5	1.6	1.0 to 2.2	3.9	2.9 to 4.9

It is to be noted that even a resolution of 2 km is coarse to model urban effects and hence the projected maximum and minimum temperatures do not take into account the impact of the Urban Heat Island (UHI), and hence the current projections of absolute temperatures may be considered as an underestimation, although there could be a much lesser impact on the projected changes. Hence, follow up studies are being

planned by CCRS that will further downscale the 2 km model simulations to 300 m (or 100 m if feasible) resolution over Singapore using the urban version of the SINGV model (uSINGV) that takes into account the urban impacts on climate variables at local scales. Daily maximum and daily minimum temperatures in Singapore are indicated by the multi-model mean to increase by at least 1°C under the low emission scenario (SSP1-2.6).

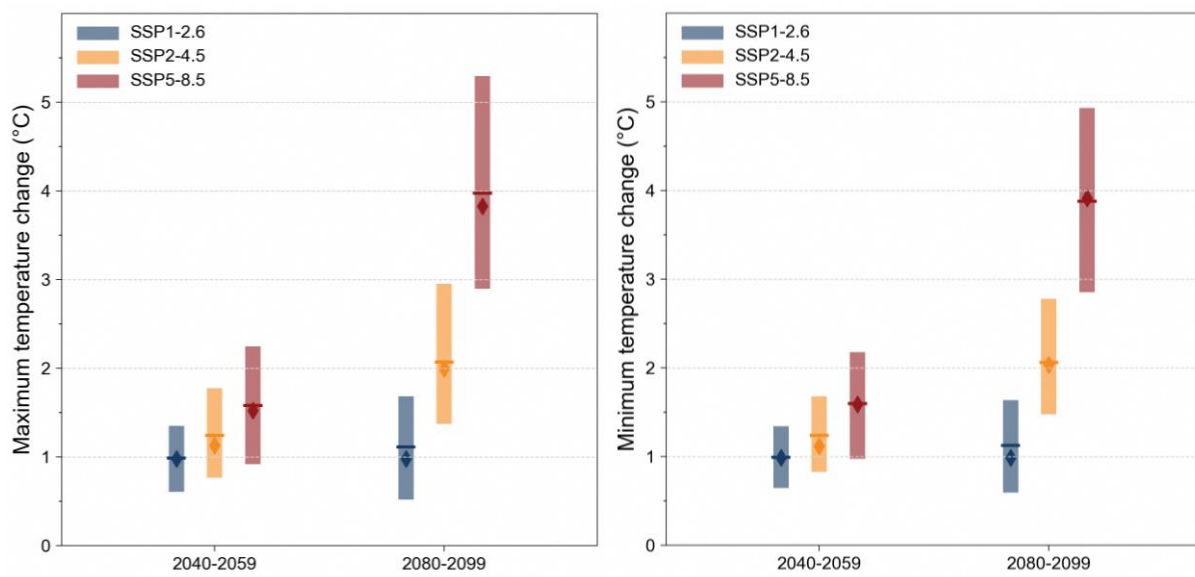


Figure 10.8: Change in mean daily minimum (tasmin) and maximum (tasmax) near-surface air temperature during mid-century (2040–2059) and end-century (2080–2099) period for the 5 bias-adjusted downscaled GCMs (2 km) over Singapore relative to the baseline (1995–2014). The line and thin diamond represent the mean and median over the 5 models, respectively. For readability, the values are available in Tables 10.21-10.22.

Temperature extremes can also be estimated using the 95th and 99.9th percentiles of the daily maximum temperatures of a region. Figure 10.9 shows the projected changes in the extreme temperature percentiles (95th & 99.9th) in the mid-century and end century under the SSP5-8.5 scenario at annual and seasonal time scales. As seen in Figure 10.9, the extreme temperatures (95th and 99.9th percentiles) are expected to increase during mid and end century under the

SSP5-8.5 at annual (Table 10.23) and seasonal time scales (Table 10.24-10.28). Towards the end of the 21st century (2100) under the SSP5-8.5 scenario, the temperature extremes are projected to significantly increase (>4°C) across annual and seasonal time scales. Based on the multi-model mean, the second inter monsoon season (ON) is expected to experience the highest increases of about 4.7°C in the extreme temperatures (95th and 99.9th percentile) at the end of the century.

Table 10.23: Projected changes in extreme temperature percentiles (ANN)

ANN	Absolute changes (SSP5-8.5) compared to historical period (°C)			
	95th Percentile		99.9th Percentile	
	Mean	Range	Mean	Range
Mid century	1.8	1.0 to 2.5	2.0	1.0 to 2.8
End century	4.4	3.0 to 5.7	4.5	3.0 to 5.9

Table 10.24: Projected changes in extreme temperature percentiles (DJ)

DJ	Absolute changes (SSP5-8.5) compared to historical period (°C)			
	95th Percentile		99.9th Percentile	
	Mean	Range	Mean	Range
Mid century	1.5	0.5 to 2.6	1.8	1.0 to 2.9
End century	4.1	3.0 to 5.3	4.3	3.0 to 5.8

Table 10.25: Projected changes in extreme temperature percentiles (FM)

FM	Absolute changes (SSP5-8.5) compared to historical period (°C)			
	95th Percentile		99.9th Percentile	
	Mean	Range	Mean	Range
Mid century	1.8	1.0 to 2.6	2.0	1.0 to 2.9
End century	4.3	2.7 to 5.8	4.5	2.9 to 6.0

Table 10.26: Projected changes in extreme temperature percentiles (AM)

AM	Absolute changes (SSP5-8.5) compared to historical period (°C)			
	95th Percentile		99.9th Percentile	
	Mean	Range	Mean	Range
Mid century	1.7	1.0 to 2.3	1.8	1.2 to 2.3
End century	4.2	3.0 to 5.3	4.3	3.0 to 5.4

Table 10.27: Projected changes in extreme temperature percentiles (ON)

ON	Absolute changes (SSP5-8.5) compared to historical period (°C)			
	95th Percentile		99.9th Percentile	
	Mean	Range	Mean	Range
Mid century	1.9	1.3 to 2.6	2.1	1.5 to 2.8
End century	4.5	3.3 to 6.0	4.7	3.3 to 6.3

Table 10.28: Projected changes in extreme temperature percentiles (JJAS)

JJAS	Absolute changes (SSP5-8.5) compared to historical period (°C)			
	95th Percentile		99.9th Percentile	
	Mean	Range	Mean	Range
Mid century	1.8	1.3 to 3.0	2.0	1.5 to 3.3
End century	4.5	3.3 to 6.0	4.5	3.0 to 6.3

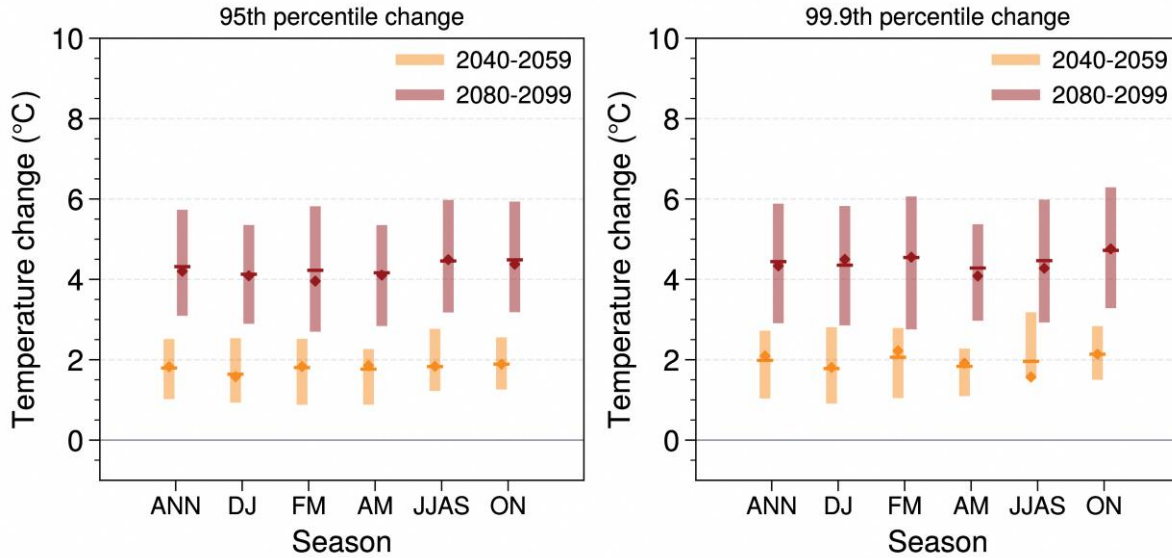


Figure 10.9: Changes in 95th and 99.9th daily maximum temperature percentile amounts for annual and various seasons from the 2-km bias-adjusted SINGV-RCM simulations during the mid- (left) and end-century (right) for SSP5-8.5. Percentiles are calculated after pooling all Singapore grid points. The line and diamond represent the mean and median using the 5 models, respectively. For readability, the values are available in Tables 10.23-10.28.

Temperature extremes of location can also be estimated using the monthly maximum of daily maximum temperatures (TXx) and monthly minimum of daily minimum temperatures (TNn). Figure 10.10 shows the multi-model mean projections of TXx over Singapore across annual and monthly timescales under the SSP5-8.5 scenario. As seen in Figure 10.10, the TXx is expected to increase on annual and monthly timescales in the end-century. The annual projections of TXx show an increase in a range of

3.3 to 4.6°C with higher range (4.4 to 4.6°C) in the western part of Singapore.

During the northeast monsoon season, for the Dec-Jan months, the TXx increases in a range of 3.2 to 4.2°C over Singapore with around 0.4°C lower in the eastern part. For the Feb-Mar months, the TXx tends to rise in a range of 3.4 to 4.8°C with higher values over western, central and northern parts.

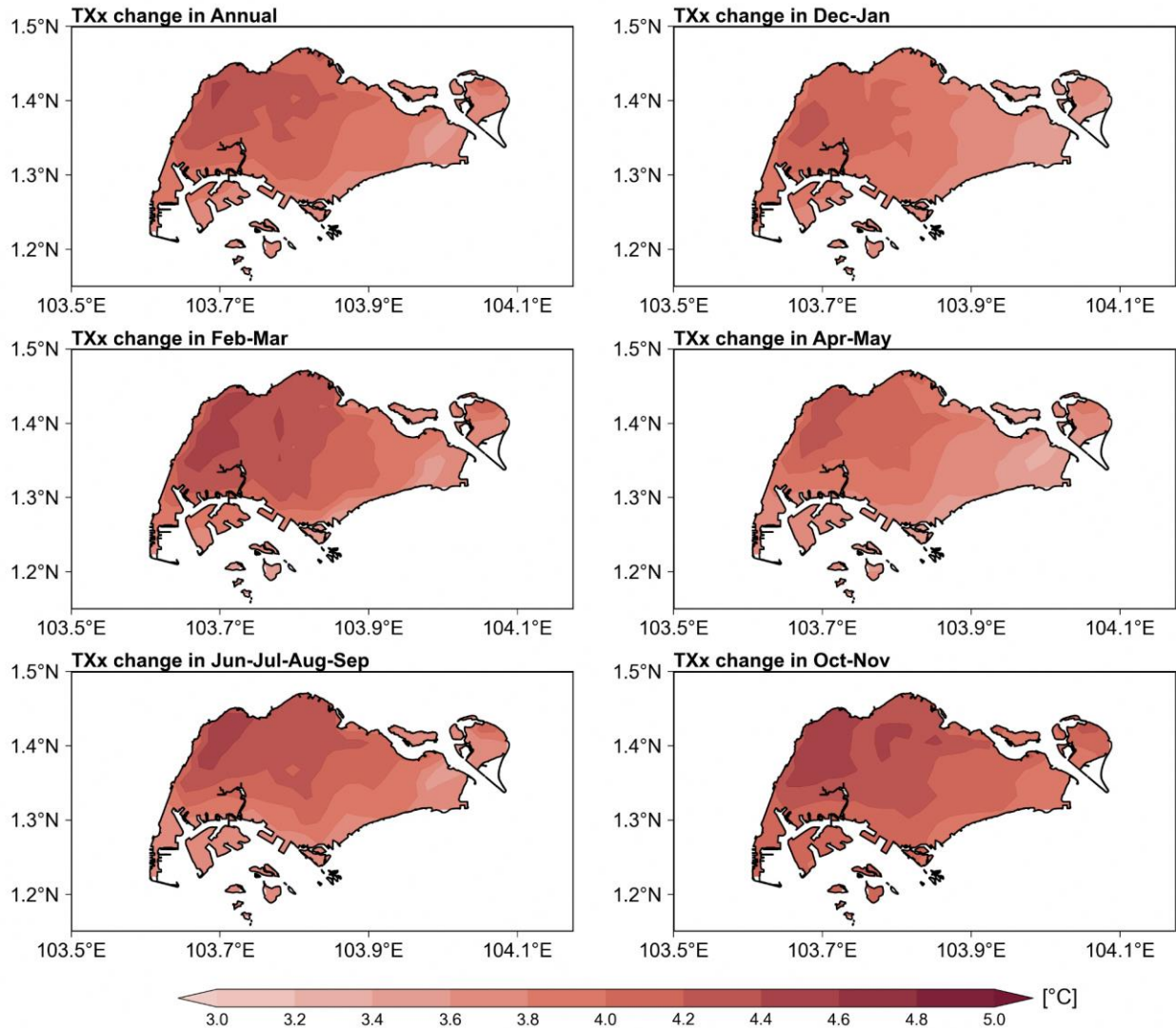


Figure 10.10: Ensemble mean (5 bias-adjusted 2km downscaled GCMs) change in monthly maximum of daily maximum temperature (TXx) for annual, December–January, February–March, April–May, June–July–August–September, and October–November during the end-century (2080–2099) period relative to the baseline (1995–2014) over Singapore under the SSP5-8.5 scenario.

During intermonsoons, for the Apr-May months, the TXx is projected to increase between 3.2 to 4.2°C. For the Oct-Nov months, the TXx is projected to increase in a range of 4.0 to 5.0°C over Singapore.

During the southwest monsoon season (Jun-Sep), the TXx is projected to increase between 3.4 to 4.8°C with a higher increase in the northern part of Singapore. According to the projections of TXx,

Oct-Nov are the months with the highest increase throughout Singapore during the end-century.

The TXx is expected to increase by 3.0 to 5.0°C with warming across Singapore at annual and seasonal time scales with higher increases over the northern, central, and western parts of Singapore. Projections for very hot days and warm nights are shown in Appendix C.

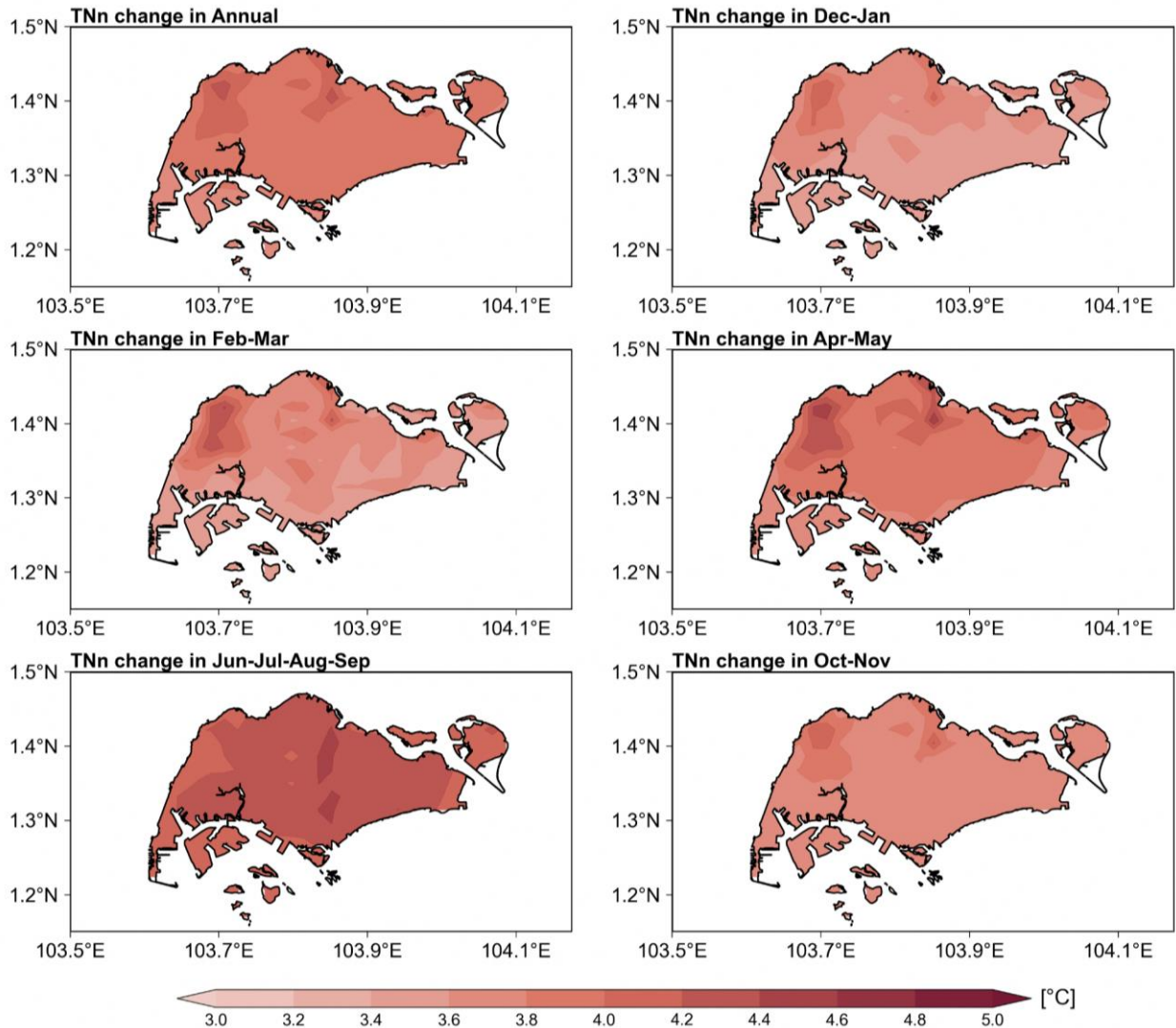


Figure 10.11: Ensemble mean (5 bias-adjusted 2km downscaled GCMs) change in monthly minimum of daily minimum temperature (TNn) for annual, December–January, February–March, April–May, June–July–August–September, and October–November during end-century (2080–2099) period relative to the baseline (1995–2014) over Singapore under the SSP5-8.5 scenario.

Figure 10.11 shows the multi-model mean projections of TNn across Singapore in the end-century under the SSP5-8.5 scenario. TNn is projected to increase on annual and monthly timescales across Singapore towards the end century under a very high emission scenario. The annual projections of TNn show an increase of 3.4 to 4.2°C.

During the northeast monsoon season, for Dec-Jan months, the TNn is projected to increase between 3.2 to 4.0°C across Singapore. For the Feb-Mar months, the TNn is projected to increase between 3.4 to 4.2°C.

During intermonsoons, for the Apr-May months, the TNn is projected to increase in a range of 3.6 to 4.8°C. For the Oct-Nov months, the TNn is projected to increase between 3.4 to 4.2°C.

During the southwest monsoons (Jun-Sep), the TNn is projected to increase between 4.0 to 5.0°C. In the end century, the TNn is projected to increase (3.2 to 5.0°C) across Singapore with higher increases over the Jun-Sep season (4.2 to 5.0°C).

Overall, the TNn is projected to increase by 3.0–5.0°C across Singapore at annual and seasonal

time scales with higher increases (>4.0°C) during the southwest monsoon season.

10.6 Changes in Heat Stress Index

According to the factsheet on Heat and Health by the UN World Health Organization, population exposure to heat is increasing due to climate change, and this trend will continue. In the backdrop of global warming, heat stress is becoming an increasingly important topic around the world, including Singapore. Although there are various metrics that can be used as indicators of heat stress, in this report we use the Wet Bulb Globe Temperature (WBGT) as a heat stress indicator and assess the future change in this indicator under 3 SSP scenarios for the mid- and end-century. Based on the hourly near-surface air temperature, wind speed, relative humidity and

net incoming solar radiation, we used Liljegren's model (Liljegren, 2008) to obtain the hourly WBGT and select the daily maximum WBGT as the heat stress indicator. The WBGT is calculated as the weighted sum of the natural wet bulb temperature T_w , the globe temperature T_g , and the dry bulb temperature T_a as:

$$WBGT = 0.7 T_w + 0.2 T_g + 0.1 T_a$$

Figure 10.12 shows the multi-model projections of WBGT under three SSP scenarios in the mid century and end century. As seen in Figure 10.12, the daily maximum WBGT is projected to increase with warming across Singapore at annual (Table 10.29) and seasonal time scales (Table 10.29-10.33). Towards the end of the current century, the annual mean daily maximum WBGT can increase by 0.5°C (SSP1-2.6) to 4.0°C (SSP5-8.5).

Table 10.29: Projected changes in annual mean daily maximum WBGT

ANN	Mid-Century (°C)		End-Century (°C)	
	Mean	Range	Mean	Range
SSP1-2.6	0.8	0.5 to 1.1	0.9	0.5 to 1.3
SSP2-4.5	1.0	0.7 to 1.4	1.7	1.2 to 2.2
SSP5-8.5	1.4	1.0 to 1.8	3.3	2.3 to 4.0

Table 10.30: Projected changes in DJ mean daily maximum WBGT

DJ	Mid-Century (°C)		End-Century (°C)	
	Mean	Range	Mean	Range
SSP1-2.6	0.8	0.6 to 1.0	0.9	0.6 to 1.3
SSP2-4.5	0.9	0.6 to 1.1	1.7	1.1 to 2.1
SSP5-8.5	1.3	0.9 to 1.8	3.1	2.1 to 3.8

Table 10.31: Projected changes in FM mean daily maximum WBGT

FM	Mid-Century (°C)		End-Century (°C)	
	Mean	Range	Mean	Range
SSP1-2.6	0.6	0.3 to 1.0	0.8	0.4 to 1.2
SSP2-4.5	1.0	0.7 to 1.3	1.4	1.0 to 1.9
SSP5-8.5	1.3	0.9 to 1.6	2.9	2.0 to 3.8

Table 10.32: Projected changes in AM mean daily maximum WBGT

AM	Mid-Century (°C)		End-Century (°C)	
	Mean	Range	Mean	Range
SSP1-2.6	0.8	0.4 to 1.1	0.9	0.4 to 1.3
SSP2-4.5	1.1	0.6 to 1.5	1.8	1.1 to 2.3
SSP5-8.5	1.3	0.8 to 1.8	3.2	2.1 to 4.1

Table 10.33: Projected changes in ON mean daily maximum WBGT

ON	Mid-Century (°C)	End-Century (°C)

	Mean	Range	Mean	Range
SSP1-2.6	0.9	0.5 to 1.2	1.0	0.5 to 1.5
SSP2-4.5	1.0	0.6 to 1.4	1.8	1.3 to 2.4
SSP5-8.5	1.8	1.3 to 2.4	3.4	2.4 to 4.1

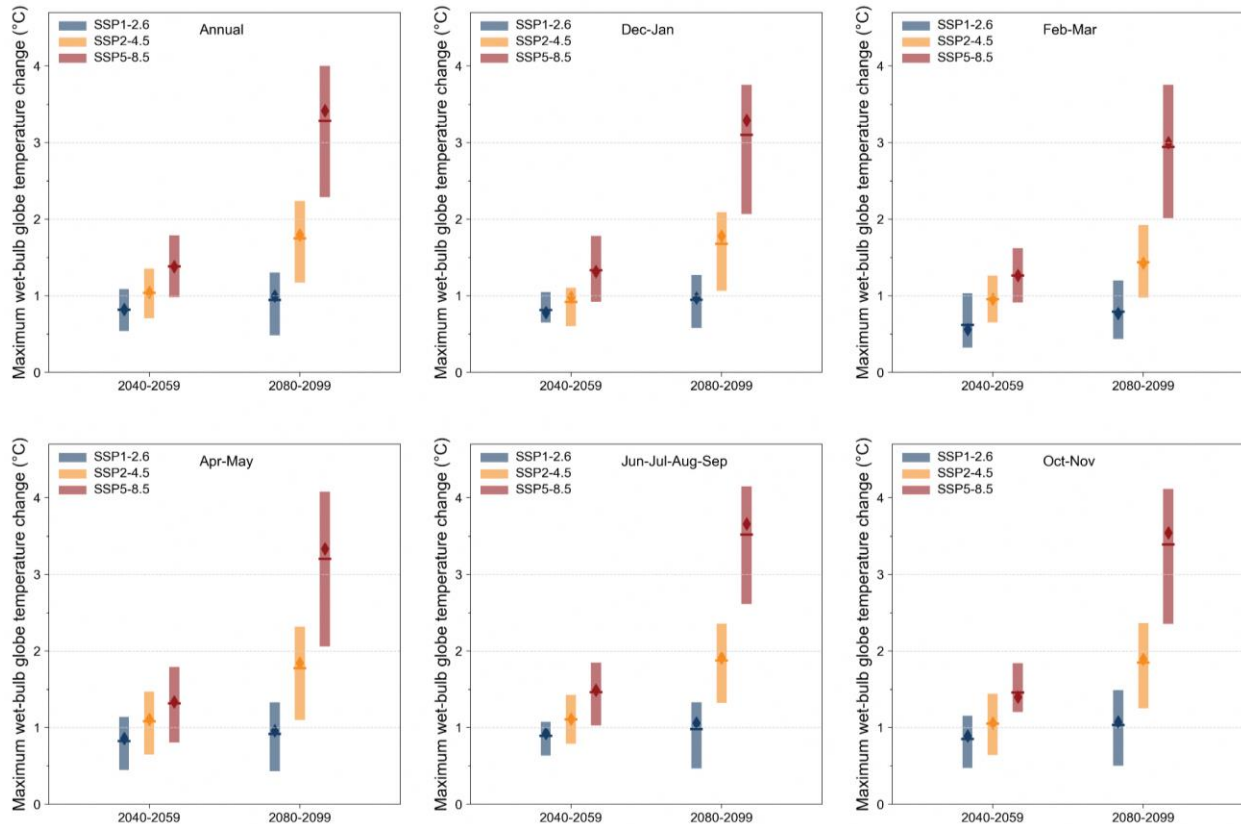


Figure 10.12: Change in daily maximum wet-bulb globe temperature (WBGT) for annual, December–January, February–March, April–May, June–July–August–September, and October–November during mid- (2040–2059) and end-century (2080–2099) periods from the 5 bias-adjusted downscaled GCMs (2 km) over Singapore relative to the baseline (1995–2014). The line and thin diamond represent the mean and median over the 5 models, respectively. For readability, the values are available in Tables 10.29–10.34.

Table 10.34: Projected changes in JJAS mean daily maximum WBGT

JJAS	Mid-Century (°C)		End-Century (°C)	
	Mean	Range	Mean	Range
SSP1-2.6	0.9	0.6 to 1.1	1.0	0.5 to 1.3
SSP2-4.5	1.1	0.8 to 1.4	1.9	1.3 to 2.4
SSP5-8.5	1.5	1.0 to 1.8	3.5	2.6 to 4.2

In the baseline period from 1995–2014, the climate models predict an annual average of 35.9 days featuring maximum WBGT above 33°C, ranging from 20.5 to 57.2 days among various models. Looking ahead, the number of days with WBGT surpassing this critical threshold is projected to rise significantly. By mid-century, under the scenarios of SSP1-2.6, SSP2-4.5 and SSP5-8.5

scenarios, we anticipate 74.9 days (ranging from 52.8 to 111.8), 87.2 days (ranging from 60.5 to 131.2), and 112.7 days (ranging from 85.8 to 154.6), respectively. The frequency of days exceeding WBGT of 33°C escalates even further, reaching 80.7 days (ranging from 54.4 to 134.6) for SSP1-2.6, 141.5 days (ranging from 107 to 204.7) for SSP2-4.5, and 269.6 days (ranging

from 207.4 to 326.1) SSP5-8.5. The projections underscore the growing heat stress challenges that lie ahead in Singapore, which requires proactive preparation for the intensified risk of heat-related illness, potential shortage of healthcare resources, and the threats to economic stability in industrial sectors relying on outdoor labors and tourism.

Figure 10.12 shows the spatial changes in the ensemble mean of monthly maximum WBGT across Singapore in the mid-century and end

century under the SSP5-8.5 scenario compared to the historical period. The WBGT is expected to rise with warming at both annual and seasonal time scales over Singapore in a range of 2.8 to 3.8°C. The southwest monsoon season (July to September) has higher WBGT increases (3.5 to 3.8°C) and the dry phase of the northeast monsoon season increases WBGT in the range of 2.8 to 3.0°C. Overall the heat stress (WBGT) which is projected to increase across Singapore in the future warmer climate can thereby influence the socio-economic conditions across the nation.

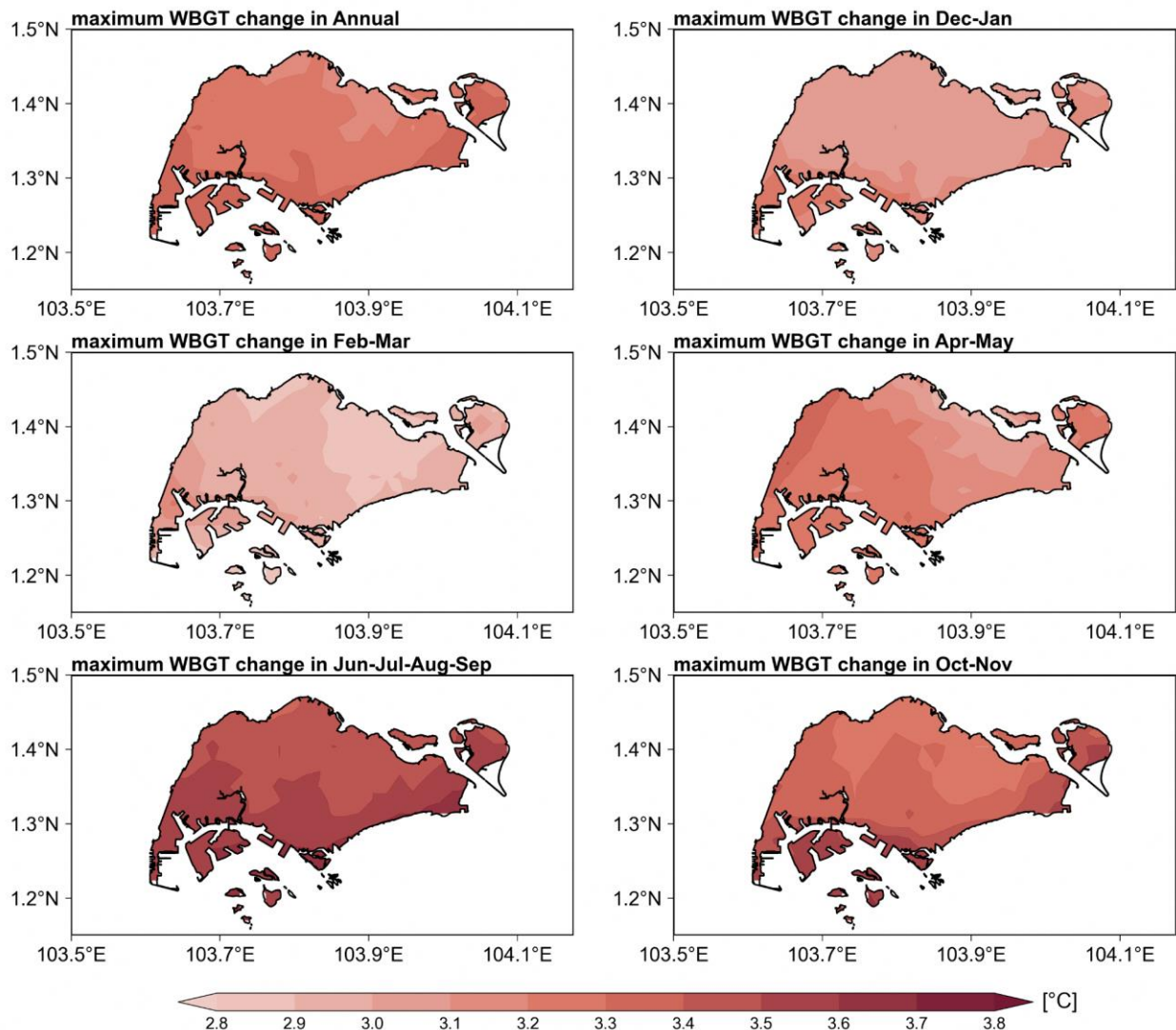


Figure 10.12: Ensemble mean (5 bias-adjusted 2km downscaled GCMs) change in monthly maximum WBGT for annual, December–January, February–March, April–May, June–July–August–September, and October–November during end-century (2080–2099) period relative to the baseline (1995–2014) over Singapore under the SSP5-8.5 scenario.

10.7 Changes in 10m relative humidity

Relative humidity is expressed as a percentage and is a measure of how saturated the air is. It

includes the combined effect of temperature and water vapour in the air. In simple terms, it is an indicator of how much water vapour the air

contains compared to the maximum it could contain at a given temperature and pressure.

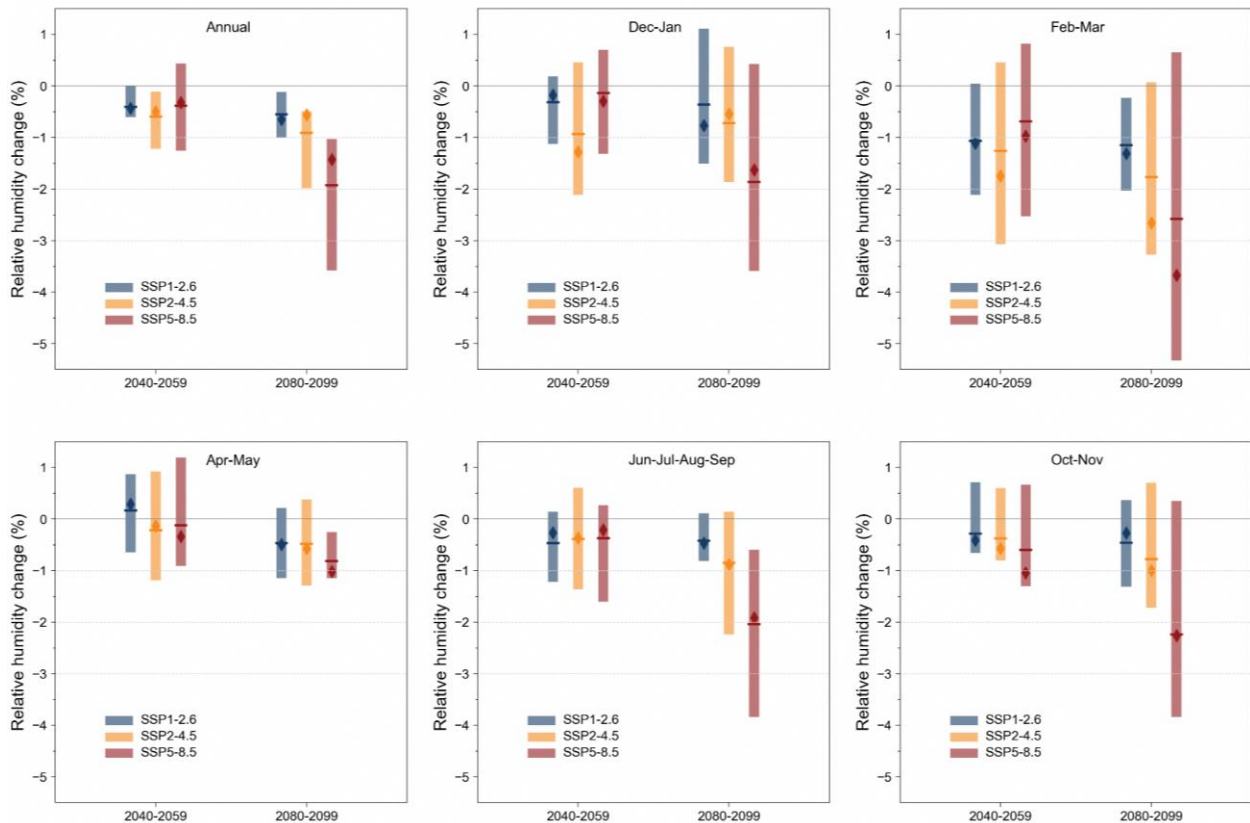


Figure 10.13: Change in mean relative humidity (hurs) for annual, December–January, February–March, April–May, June–July–August–September, and October–November during mid- (2040–2059) and end-century (2080–2099) periods for the 5 bias-adjusted downscaled GCMs (2 km) over Singapore relative to the baseline (1995–2014). The line and thin diamond represent the mean and median over the 5 models, respectively. For readability, the values are available in Tables 10.35-10.40.

With increase in temperature, the amount of water vapour in the air is expected to increase. This is because of the Clausius-Clapeyron (CC) equation, which implies that the air can generally hold around 7% more moisture for every 1°C increase in air temperature. Therefore, under global warming, for the relative humidity to be constant the water vapour content in the air should increase at the same rate i.e., 7% increase for every 1°C increase in air temperature. However, from Singapore’s observation records we find that there is a decreasing trend in relative humidity. This also matches with what was projected in V2. The reasons for this is (1) there is a limited supply of moisture in the land unlike oceans, and (2) the land surface has been warming at a faster rate than oceans. Hence, neither the local evaporation

over land, nor the advected moisture from the oceans is enough to increase the water vapour over land at the CC rate.

Figure 10.13 shows the multi-model mean projections of RH under three SSP scenarios in the mid and end century at annual and seasonal time scales. As seen in Figure 10.13, the RH is projected to decrease over Singapore at annual and seasonal time scales in mid century and end century. Towards the end of the century, the annual mean RH is projected to decrease by 0.5% (SSP1-2.6) to 1.9% (SSP5-8.5). When compared to other seasons, the northeast monsoon dry phase (Feb-Mar) project decreased RH by 1.2% (SSP1-2.6) and 2.6% (SSP5-8.5) in the end century. Additionally, the projected changes in RH

during the dry phase of the northeast monsoon show significant inter-model variation.

Table 10.35: Projected changes in annual mean RH

ANN	Mid-Century (%)		End-Century (%)	
	Mean	Range	Mean	Range
SSP1-2.6	-0.4	-0.6 to 0.0	-0.5	-1.2 to -0.1
SSP2-4.5	-0.6	-1.2 to -0.1	-0.9	-2.0 to -0.5
SSP5-8.5	-0.4	-1.3 to 0.4	-1.9	-3.6 to -1.0

Table 10.36: Projected changes in DJ mean RH

DJ	Mid-Century (%)		End-Century (%)	
	Mean	Range	Mean	Range
SSP1-2.6	-0.3	-1.1 to 0.2	-0.4	-1.5 to 1.1
SSP2-4.5	-0.9	-2.1 to 0.5	-0.7	-1.9 to 0.8
SSP5-8.5	-0.1	-1.3 to 0.7	-1.9	-3.6 to 0.4

Table 10.37: Projected changes in FM mean RH

FM	Mid-Century (%)		End-Century (%)	
	Mean	Range	Mean	Range
SSP1-2.6	-1.1	-2.1 to 0.0	-1.2	-2.0 to -0.2
SSP2-4.5	-1.3	-3.1 to 0.5	-1.8	-3.3 to 0.1
SSP5-8.5	-0.7	-2.5 to 0.8	-2.6	-5.3 to 0.7

Table 10.38: Projected changes in AM mean RH

AM	Mid-Century (%)		End-Century (%)	
	Mean	Range	Mean	Range
SSP1-2.6	0.2	-0.6 to 0.9	-0.5	-1.1 to 0.2
SSP2-4.5	-0.2	-1.2 to 0.9	-0.5	-1.3 to 0.4
SSP5-8.5	-0.1	-0.9 to 1.2	-0.8	-1.1 to -0.3

Table 10.39: Projected changes in ON mean RH

ON	Mid-Century (%)		End-Century (%)	
	Mean	Range	Mean	Range
SSP1-2.6	-0.3	-0.7 to 0.7	-0.5	-1.3 to 0.4
SSP2-4.5	-0.4	-0.8 to 0.6	-0.8	-1.7 to 0.7
SSP5-8.5	-0.6	-1.3 to 0.7	-2.2	-3.9 to 0.3

Table 10.40: Projected changes in JJAS mean RH

ANN	Mid-Century (%)		End-Century (%)	
	Mean	Range	Mean	Range
SSP1-2.6	-0.5	-1.2 to 0.7	-0.5	-1.3 to 0.4
SSP2-4.5	-0.4	-1.4 to 0.6	-0.9	-2.2 to 0.1
SSP5-8.5	-0.4	-1.6 to 0.3	-2.0	-3.8 to -0.6

10.8 Changes in 10m wind speed

This section presents the annual cycle of mean surface wind speeds in the historical and 2 km downscaled SINGV simulations under the SSP5-8.5 scenario in the mid and end century. We also present the projected changes in the mean surface wind speed for three SSP scenarios at annual and seasonal time scales in mid and end century.

Figure 10.14 shows the annual cycle of surface wind speeds over Singapore during historical,

mid-century (SSP5-8.5), and end-century (SSP5-8.5). In all three time periods, the annual cycle comprises higher wind speeds in the northeast and southwest monsoon seasons and lower wind speeds in the intermonsoon seasons. Relative to the historical simulations, there is not much change in the mid-century for most of the year, but by the end of the century, the mean surface wind speeds exceed those of historical throughout the year, especially in Jan-Sep, where there is high model agreement on the increases.

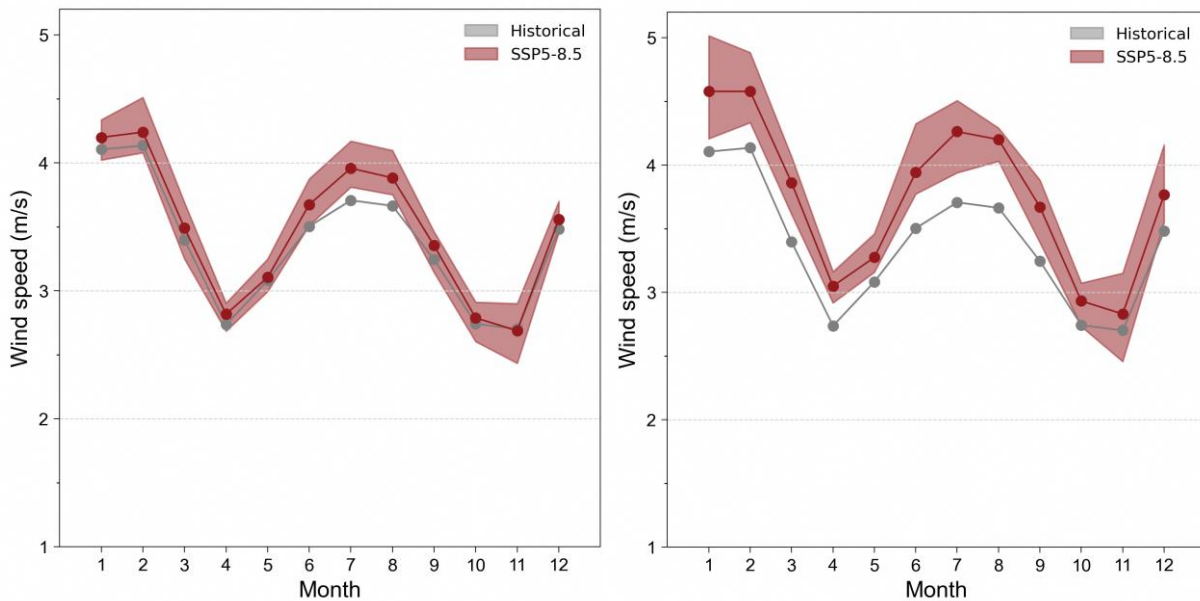


Figure 10.14: Annual cycle of historical and future winds under mid- (left) and end-century (right).

Projected changes in surface wind speed for mid- and end-century under the 3 SSP scenarios are shown in Figure 10.15. As seen in the figure, projected mean surface wind speed changes over Singapore varies on annual (Table 10.41) and monthly scales (Table 10.42-10.46). At annual time scales, the mean wind speeds are projected

to increase by 0.1 m/s (SSP1-2.6) to 0.37 m/s (SSP5-8.5). Under the SSP5-8.5 scenario, the northeast monsoon and southwest monsoon seasons are projected to experience greater increases in mean wind speeds in the end of the century.

Table 10.41: Projected changes in annual mean 10m wind speed

ANN	Mid-Century (m/s)		End-Century (m/s)	
	Mean	Range	Mean	Range
SSP1-2.6	0.10	0.02 to 0.16	0.10	0.0 to 0.17
SSP2-4.5	0.12	0.03 to 0.19	0.19	0.09 to 0.28
SSP5-8.5	0.10	-0.03 to 0.24	0.37	0.23 to 0.51

Table 10.42: Projected changes in DJ mean 10m wind speed

DJ	Mid-Century (m/s)		End-Century (m/s)	
	Mean	Range	Mean	Range

SSP1-2.6	0.03	-0.05 to 0.20	0.09	-0.06 to 0.22
SSP2-4.5	0.14	-0.02 to 0.31	0.16	0.00 to 0.36
SSP5-8.5	0.08	-0.05 to 0.22	0.38	0.09 to 0.80

Table 10.43: Projected changes in FM mean 10m wind speed

FM	Mid-Century (m/s)		End-Century (m/s)	
	Mean	Range	Mean	Range
SSP1-2.6	0.18	0.00 to 0.43	0.14	-0.02 to 0.33
SSP2-4.5	0.16	0.01 to 0.33	0.33	0.07 to 0.54
SSP5-8.5	0.10	-0.10 to 0.33	0.45	0.21 to 0.70

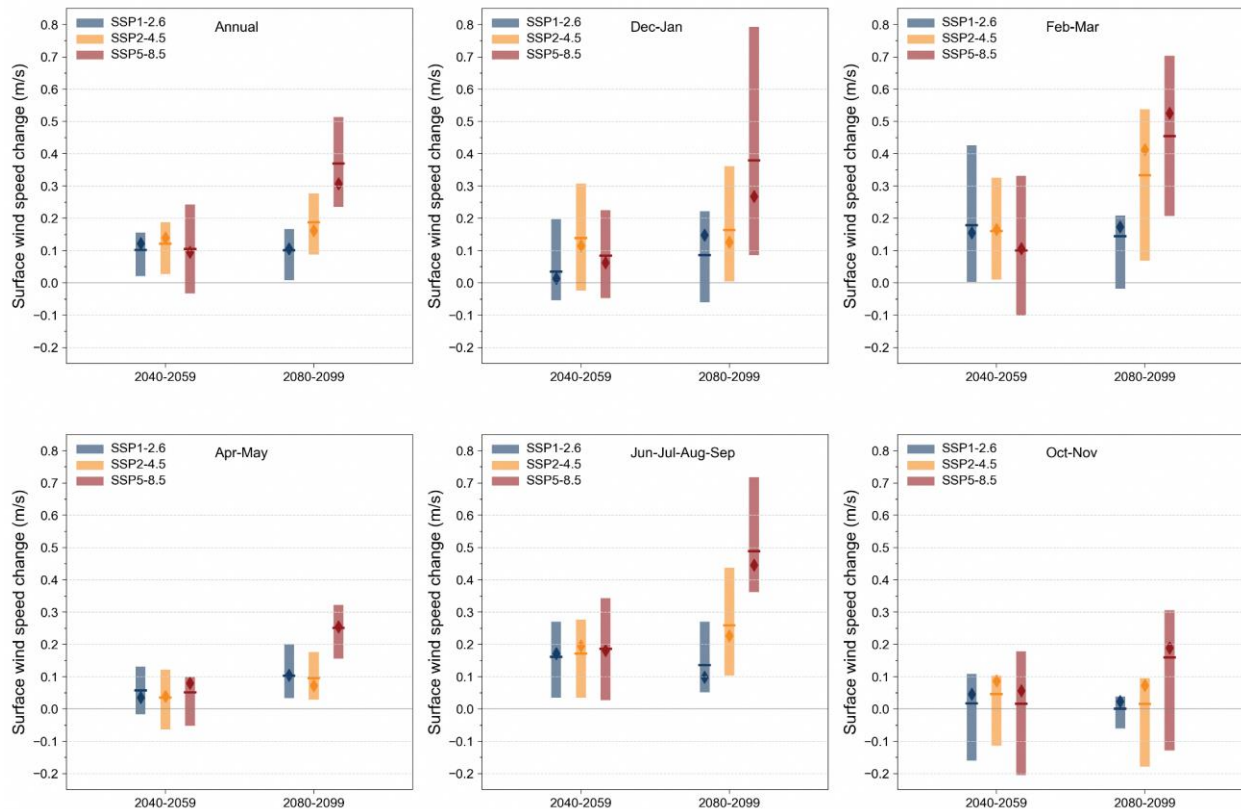


Figure 10.15: Changes in mean 10m wind speed for annual, December–January, February–March, April–May, June–July–August–September, and October–November during mid- (2040–2059) and end-century (2080–2099) periods for the 5 bias-adjusted downscaled GCMs (2 km) over Singapore relative to the baseline (1995–2014). The line and thin diamond represent the mean and median over the 5 models, respectively. For readability, the values are available in Tables 10.41–10.46.

Table 10.44: Projected changes in AM mean 10m wind speed

AM	Mid-Century (m/s)		End-Century (m/s)	
	Mean	Range	Mean	Range
SSP1-2.6	0.06	-0.02 to 0.13	0.10	0.03 to 0.20
SSP2-4.5	0.04	-0.06 to 0.12	0.10	0.03 to 0.18
SSP5-8.5	0.05	-0.05 to 0.10	0.25	0.16 to 0.32

Table 10.45: Projected changes in ON mean 10m wind speed

ON	Mid-Century (m/s)		End-Century (m/s)	
	Mean	Range	Mean	Range
SSP1-2.6	0.06	-0.02 to 0.13	0.10	0.03 to 0.20
SSP2-4.5	0.04	-0.06 to 0.12	0.10	0.03 to 0.18
SSP5-8.5	0.05	-0.05 to 0.10	0.25	0.16 to 0.32

SSP1-2.6	0.02	-0.16 to 0.11	0.0	-0.06 to 0.04
SSP2-4.5	0.05	-0.11 to 0.10	0.01	-0.19 to 0.09
SSP5-8.5	0.02	-0.20 to 0.18	0.16	-0.13 to 0.31

Table 10.46: Projected changes in JJAS mean 10m wind speed

JJAS	Mid-Century (m/s)		End-Century (m/s)	
	Mean	Range	Mean	Range
SSP1-2.6	0.16	0.03 to 0.27	0.14	0.05 to 0.27
SSP2-4.5	0.17	0.03 to 0.28	0.26	0.10 to 0.44
SSP5-8.5	0.19	0.03 to 0.34	0.49	0.36 to 0.72

10.9 Changes in Wind Gusts

In this section, we present the projected changes in daily maximum wind gust under warming. Strong wind gusts are often associated with thunderstorms and squall lines and can potentially cause substantial damage to Singapore’s infrastructure (buildings and roads), uprooting of trees, and threat to the safety of human beings. While in V2, due to the use of a coarser spatial resolution model (12km grid size), thunderstorms and squall lines could not be simulated well. Hence, wind gust changes were projected using a single model run at 1.5km resolution for the last decade of the 21st century for the RCP8.5 scenario. In V3 there is a significant improvement

in the simulation of the processes causing strong wind gusts due to the use of an advanced numerical model (SINGV-RCM) and higher resolution (2km), and we have more confidence in the wind gust projections.

Figure 10.16 shows the spatial distribution of multi-model mean of the percentages changes in the wind gust speed in the mid- and end-century from the 2 km simulations under SSP5-8.5. It can be seen from the figure that the increase in mid-century is less than 3%, and that during the end-century is less than 10%. This is consistent with the projections from V2 that showed a future end-century increase under RCP8.5 by 5-10%.

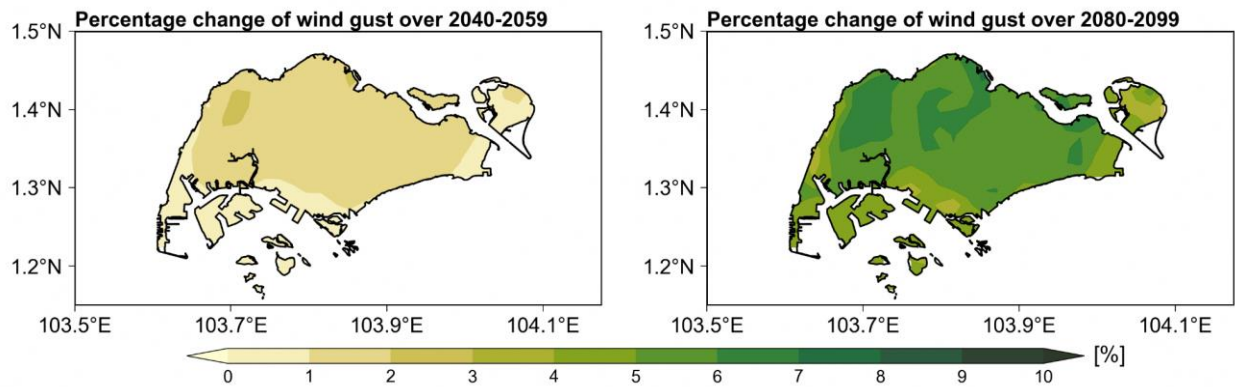


Figure 10.16: Ensemble mean (5 bias-adjusted 2km downscaled GCMs) percentage change in wind gust (10m daily maximum wind speed) during mid- (2040–2059) and end-century (2080–2099) relative to the baseline (1995–2014) over Singapore under SSP5-8.5 scenario.

10.10 Comparison of 2km and 8km Projections

In this section we compare the projections of rainfall and temperature over Singapore from the

bias-adjusted 8km and 2km downscaled simulations. For brevity, we present results only

for temperature and rainfall and for the SSP5-8.5 scenario.

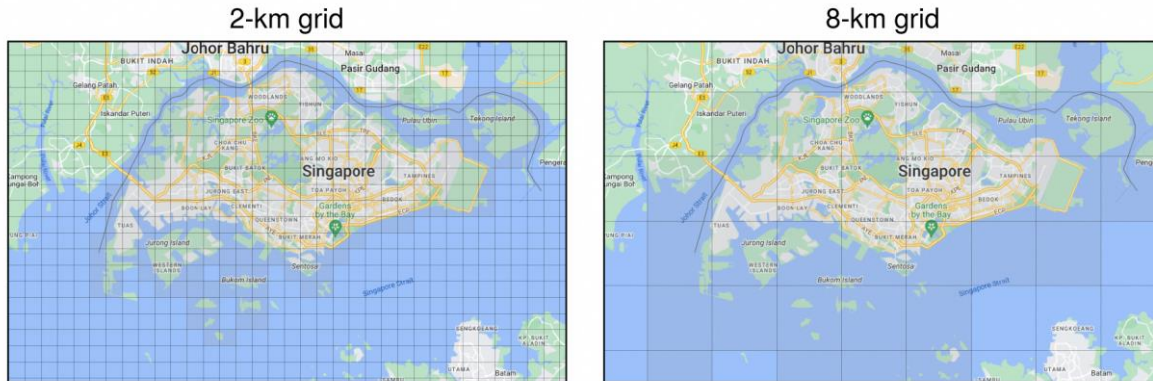


Figure 10.17: The two SINGV-RCM grids over the Singapore region. (Left) 2-km grid. (Right) 8-km grid.

While we are making this comparison only over Singapore (25 grid points in the 8km model and 286 grid points in the 2km model), results over the broader region could be more similar due to the fact that the 8km model provides the driving conditions and hence large-scale constraints for the 2km simulations. Also, the 2km simulations can better resolve some of the local climate drivers such as squall lines, thunderstorms, and land-sea breeze circulation, so we would expect improved rainfall projections, especially extremes.

The multi-model annual and seasonal mean rainfall and temperature projections over Singapore using 2 km and 8 km downscaled GCM simulations during the end century under SSP5-8.5 scenario were analysed (figures in Appendix A). It was found that the 2 km and 8 km projections largely agree both in magnitude and spatial pattern, although one may find small local variations and higher spatial granularity in the 2 km simulations due to the higher resolution. Although the local variations may appear small, aggregated together in space they could lead to larger differences between the 8 km and the 2 km projections. For example, as can be seen in Fig A10.3, the percentage change in 99.9th percentile projected in the 8 km simulations is ~10% whereas that in the 2 km projections is ~40%.

This chapter uses bias-adjusted projections of 6 CMIP6 GCMs downscaled by SINGV-RCM to examine climate change over Singapore. The results are presented for both annual and seasonal scales, using periods corresponding to Singapore’s monsoon and intermonsoon seasons. Changes in rainfall, temperature, wet bulb globe temperature as a measure of what stress, relative humidity, and near-surface winds and wind gusts are presented.

Multi-model annual mean rainfall is projected to remain the same or increase by the end of the century over Singapore (11% across scenarios), although there are individual models that project reductions in rainfall. Similar to the regional case, the changes in annual means are not uniformly distributed over seasons. In the case of SSP5-8.5, by the end-century, there are signs of greater contrasts between the wet (e.g. Dec-Jan), and dry (e.g. Feb-Mar, Jun-Sep), or a ‘wet-get-wetter’ and ‘dry-get-drier’ type behavior.

In the end of the century under SSP5-8.5, there are generally increases in precipitation extremes as measured by annual maximum 1-day and 5-day precipitation (RX1day and RX5day) of up to 50% across different seasons. The main exception is Feb-Mar, where large parts of Singapore show a decrease in both RX1day and RX5day. Models project an increase across seasons in the 99.9th percentile of rainfall in both mid-century and end-century in SSP5-8.5. The multi-model mean length of dry spells (measured by consecutive dry days) increases in all

10.11 Summary

scenarios in both the mid-century and end-century periods.

Annual mean near-surface air temperatures are projected to increase in a range of 0.6-5.0°C by the end of the century under SSP5-8.5. Models robustly agree on an increase in temperature across all seasons, with all seasons showing similar increases in temperature. Annual mean daily maximum temperatures are also projected to increase across models, with a range of 0.5-5.3°C. Annual average daily mean wet-bulb globe temperature is projected to increase in the range of 0.5-4.3°C. There is also a decrease in multi-model mean near-surface relative humidity. The reduction in relative humidity has a compensating effect on enhanced heat stress under warming.

No major changes are expected in wind-related variables. Changes in near-surface winds are generally small (within 1 m/s). By the end of the century, the multi-model mean winds are

expected to increase in all seasons under SSP5-8.5. Changes in wind gusts are expected to be within 10% under SSP5-8.5, even up till the end of the century.

A discussion of the comparison of the 2km and 8km simulations indicate that the spatial pattern simulated by the model at the two resolutions are broadly similar, but the differences can lead to noticeable differences in domain-wide statistics. In this case, we would tend to trust the 2km model, which at a higher resolution is better able to resolve key physical processes which drive and organize convection.

In summary, the models predict increases in temperature and heat stress over Singapore, together with greater variability of rainfall and rainfall extremes. This includes greater occurrences and duration of drought conditions, as well as increases in extreme rainfall.

References

- WHO (2020) <https://www.who.int/news-room/fact-sheets/detail/climate-change-heat-and-health>
- Bui, H. X., Li, Y.-X., Maloney, E. D., Kim, J.-E., Lee, S.-S., & Yu, J.-Y. (2023). Emergence of Madden-Julian oscillation precipitation and wind amplitude changes in a warming climate. *Npj Climate and Atmospheric Science*, 6(1), 1–6. <https://doi.org/10.1038/s41612-023-00344-z>
- Byrne, M. P., & Schneider, T. (2016). Narrowing of the ITCZ in a warming climate: Physical mechanisms. *Geophysical Research Letters*, 43(21), 11,350–11,357. <https://doi.org/10.1002/2016GL070396>
- Cai, W., Borlace, S., Lengaigne, M., van Rensch, P., Collins, M., Vecchi, G., et al. (2014). Increasing frequency of extreme El Niño events due to greenhouse warming. *Nature Climate Change*, 4(2), 111–116. <https://doi.org/10.1038/nclimate2100>
- Cai, W., Santoso, A., Collins, M., Dewitte, B., Karamperidou, C., Kug, J.-S., et al. (2021). Changing El Niño–Southern Oscillation in a warming climate. *Nature Reviews Earth & Environment*, 1–17. <https://doi.org/10.1038/s43017-021-00199-z>
- Chen, C., Sahany, S., Moise, A. F., Chua, X. R., Hassim, M. E., Lim, G., & Prasanna, V. (2023). ENSO-rainfall teleconnection over the Maritime Continent enhances and shifts eastward under warming. *Journal of Climate*, 1(aop), 1–55. <https://doi.org/10.1175/JCLI-D-23-0036.1>
- Geng, T., Cai, W., Wu, L., Santoso, A., Wang, G., Jing, Z., et al. (2022). Emergence of changing Central-Pacific and Eastern-Pacific El Niño–Southern Oscillation in a warming climate. *Nature Communications*, 13(1), 6616. <https://doi.org/10.1038/s41467-022-33930-5>
- Ghosh, R., & Shepherd, T. G. (2023). Storylines of Maritime Continent dry period precipitation changes under global warming. *Environmental Research Letters*, 18(3), 034017. <https://doi.org/10.1088/1748-9326/acb788>
- James C. Liljegren, Richard A. Carhart, Philip Lawday, Stephen Tschopp & Robert Sharp (2008). Modeling the Wet Bulb Globe Temperature Using Standard Meteorological Measurements. *Journal of Occupational and Environmental Hygiene*, 5:10, 645–655, <https://doi.org/10.1080/15459620802310770>
- Johnson, N. C., Amaya, D. J., Ding, Q., Kosaka, Y., Tokinaga, H., & Xie, S.-P. (2020). Multidecadal modulations of key metrics of global climate change. *Global and Planetary Change*, 188, 103149. <https://doi.org/10.1016/j.gloplacha.2020.103149>
- Lange, S. (2019). Trend-preserving bias adjustment and statistical downscaling with ISIMIP3BASD (v1.0). *Geoscientific Model Development*, 12(7), 3055–3070. <https://doi.org/10.5194/gmd-12-3055-2019>
- Liang, J., Catto, J. L., Hawcroft, M., Hodges, K. I., Tan, M. L., & Haywood, J. M. (2021). Climatology of Borneo Vortices in the HadGEM3-GC3.1 General Circulation Model. *Journal of Climate*, 34(9), 3401–3419. <https://doi.org/10.1175/JCLI-D-20-0604.1>
- Liang, J., Tan, M. L., Catto, J. L., Hawcroft, M. K., Hodges, K. I., & Haywood, J. M. (2022). Projected near-term changes in monsoon precipitation over Peninsular Malaysia in the HighResMIP multi-model ensembles. *Climate Dynamics*. <https://doi.org/10.1007/s00382-022-06363-5>

Appendix A - Comparison of Rainfall and Temperature Changes in the 8km and 2km projections

Rainfall

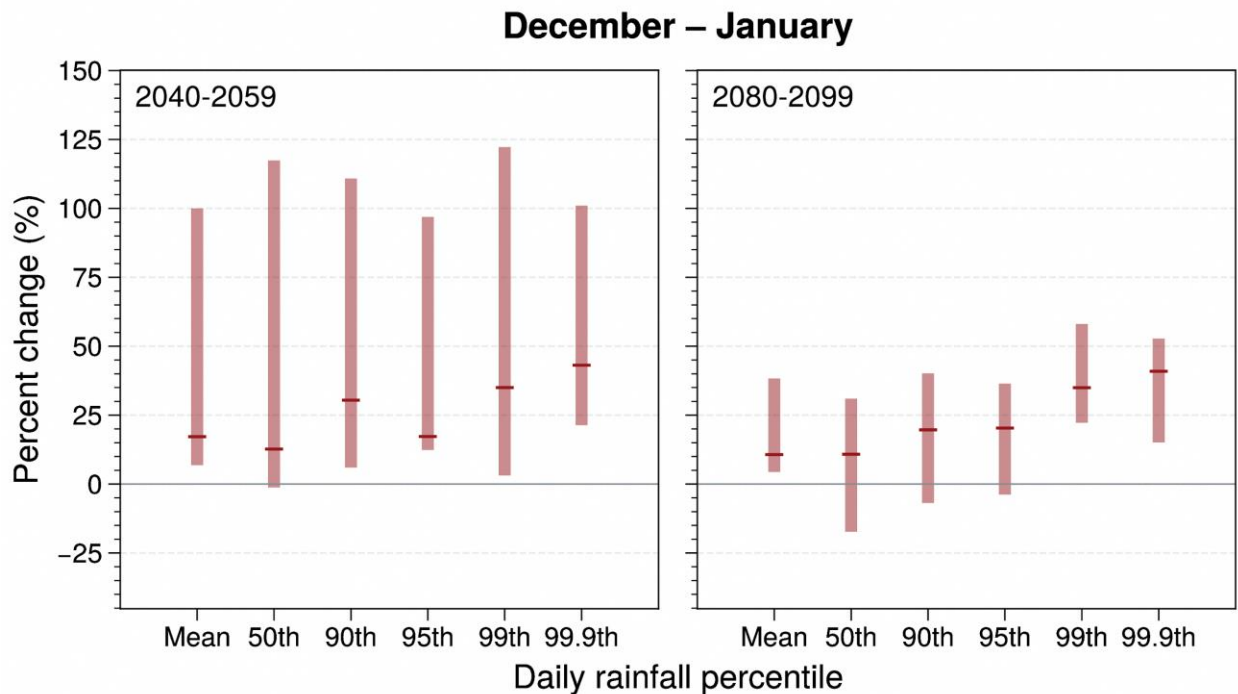
Figure A10.1 shows the spatial mean projections of daily mean and extreme rainfall percentiles over Singapore in the mid and end century on annual and seasonal time scales.

For the Dec-Jan months, the mid-century projections of mean rainfall show an increase of 17% and extreme rainfall percentiles increase with a range of (12-40%). In the end century, the daily mean rainfall projections show an increase of 10% and extreme rainfall increase with a range of (11-35%). During the Feb-Mar months, in the mid-century the mean rainfall increases by 25% and extreme rainfall shows an increasing trend with a range of (0-38%). In the end century, the projections of the mean rainfall shows neutral

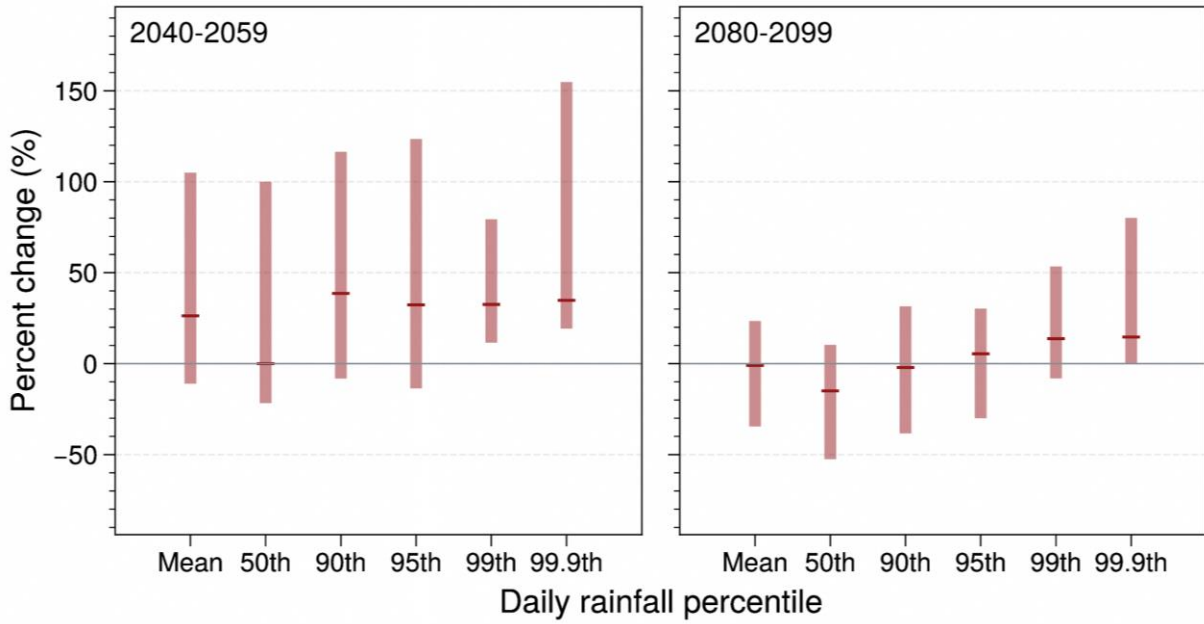
changes and extreme rainfall varies with a range of (-20-15%).

During the Apr-May months, the projections of daily mean rainfall increases by 5% and extreme rainfall rises with a range of (3-20%). In the end century, the mean rainfall increases by 17% and extreme rainfall increases with a range of 0-50%. For the Jun-Sep period, the mid-century projections of the mean show an increase of 5% and extreme rainfall varies with a range of (-4-30%). In the end century, mean rainfall increases by 15% and extreme rainfall projections vary with a range of (-4 to 26%).

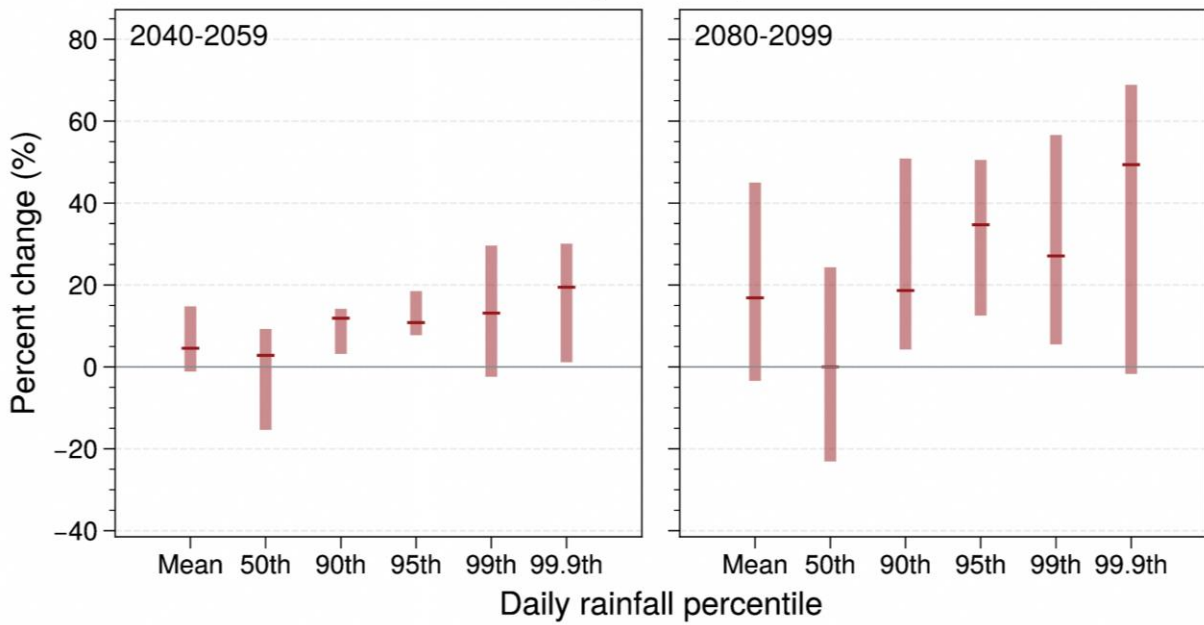
During the Oct-Nov months, in the mid-century mean rainfall increases by 9% and extreme rainfall increases with a range of (5-26%). Over the end century, mean rainfall rises by 14% and extreme rainfall enhances with a range of (5-60%). These results suggest that there are variations in the projections of the daily mean and extreme rainfall of Singapore in the mid-century and the end century across annual and monthly timescales.



February – March



April – May



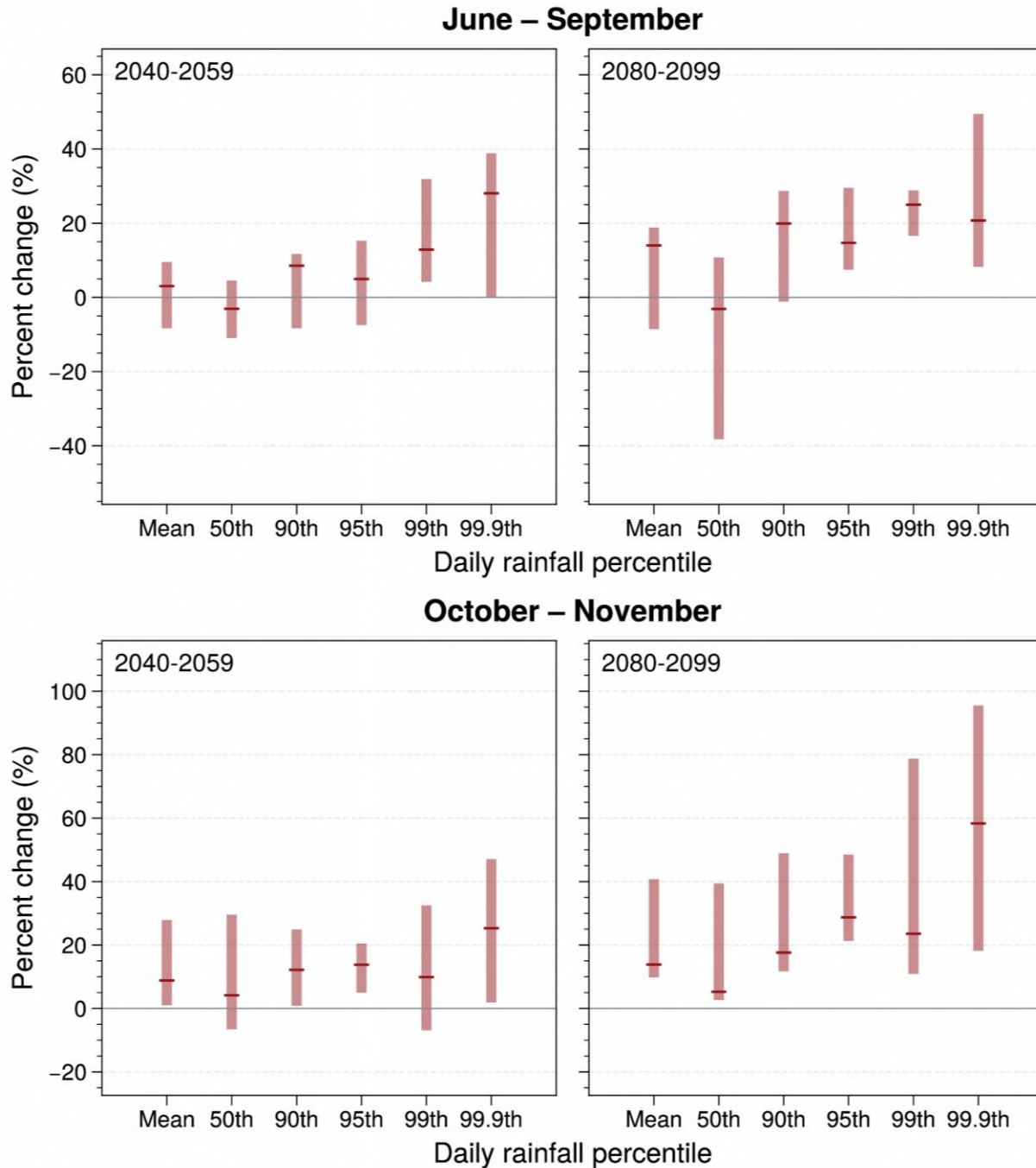


Figure A10.1: Range of percentage changes in mean and extreme daily rainfall percentile amounts for various seasons (December-January, wet NE monsoon; February-March, dry NE monsoon; April-May, first intermonsoon; June-September; SW monsoon) from the 2-km SINGV-RCM simulations over Singapore. The median value in the range of percentage changes for each percentile is denoted by the dark red horizontal line. Rainfall percentiles are based on wet days only (defined as any day when rainfall ≥ 1 mm/day); each percentile uses the nearest corresponding daily rainfall value.

As seen in Figure A10.2 the mean and extremes are projected to rise in the mid-century but with a higher magnitude in the end century.

Temperature

For the Dec-Jan months, the daily maximum mean temperatures are expected to increase by 1.4 degrees and extremes increase with a range of 1.3 to 1.7 degrees in the mid century. In the end century, the mean daily maximum

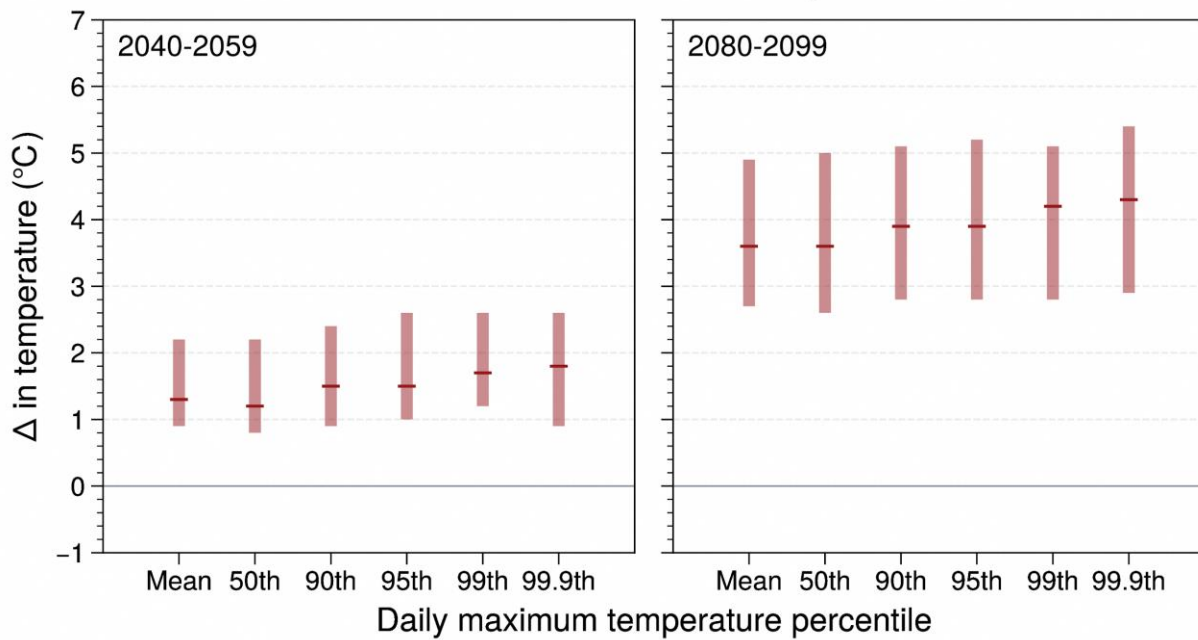
temperatures are projected to increase by 3.6 degrees and extremes increase with a range of 3.6 to 4.4 degrees. During Feb-Mar months, in the mid-century the mean daily maximum temperatures are projected to increase by 1.5 degrees and extremes increase with a range of 1.4 to 1.8 degrees. In the end century, the mean temperatures are projected to increase by 3.5 degrees and extremes increase with a range of 3.5 to 4.2 degrees.

During the Apr-May months, the mean temperatures are expected to increase by 1.6 degrees and extremes increase with a range of 1.6 to 1.8 degrees. In the end century the mean temperatures are projected to rise by 3.6 degrees

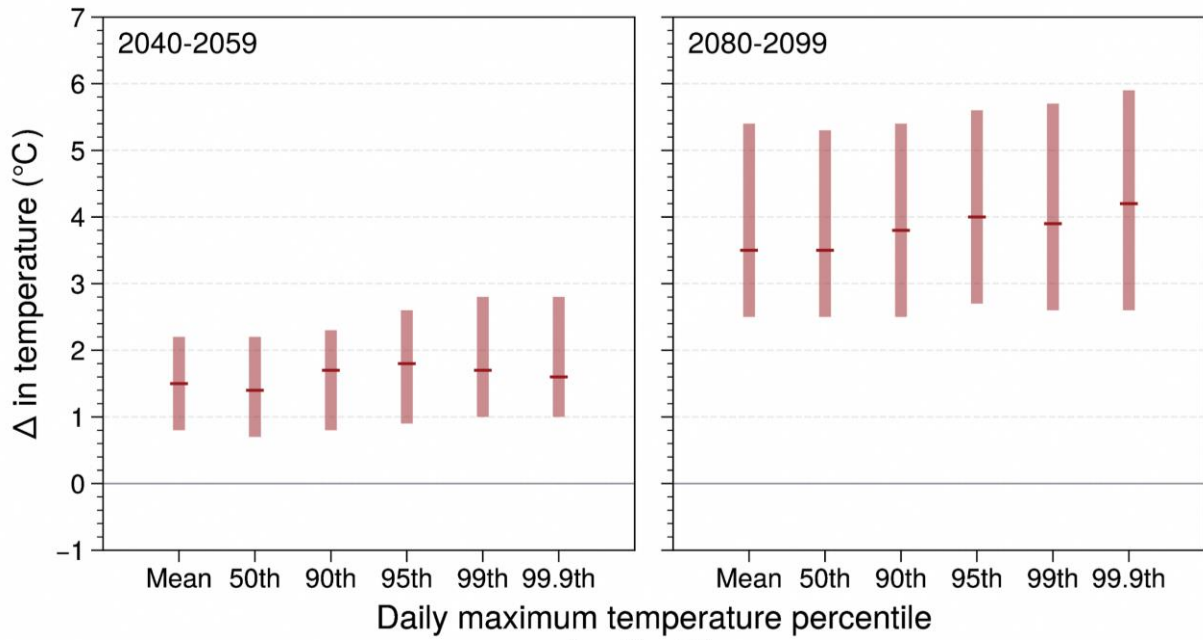
and extremes increase with a range of 3.6 to 4.1 degrees. For the Jun-Sep period, in the mid-century the mean temperatures are expected to rise by 1.6 degrees and extremes increase with a range of 1.5 to 1.7 degrees. In the end century, the mean temperatures projected to increase by 4.1 degrees and extremes increase with a range 4.1 to 4.4 degrees.

During the Oct-Nov months, in the mid-century the mean temperatures are projected to increase by 1.6 degrees and extremes increase with a range of 1.5 to 1.9 degrees. In the end century, the mean temperatures are expected to rise by 4 degrees and extremes increase with a range of 4.0 to 4.5 degrees.

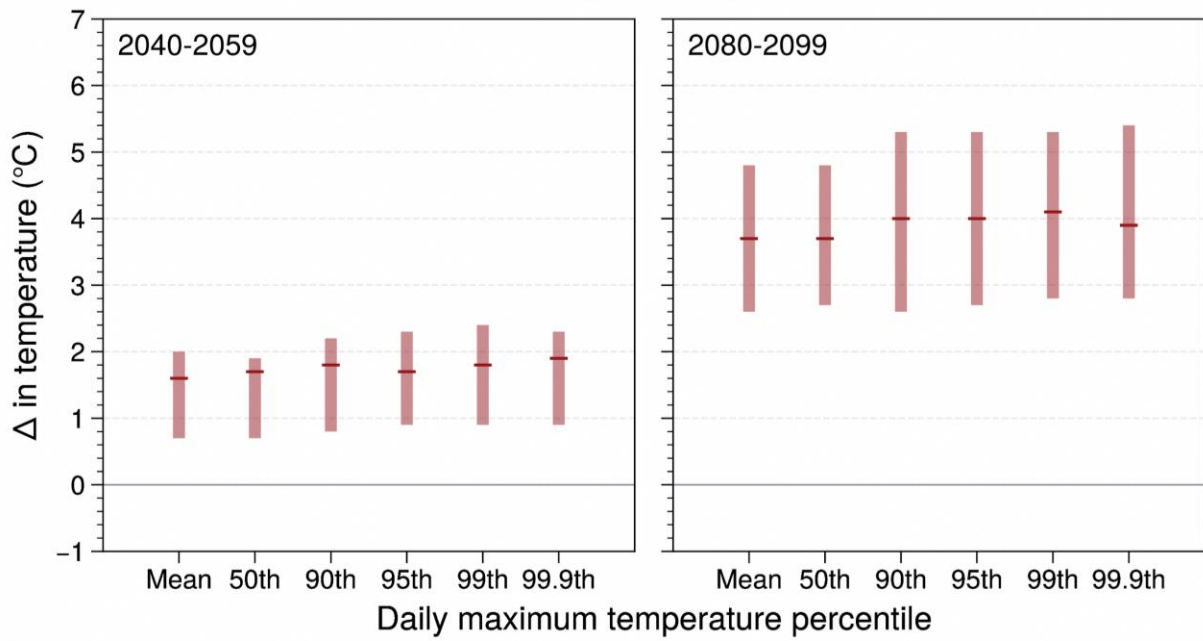
December – January



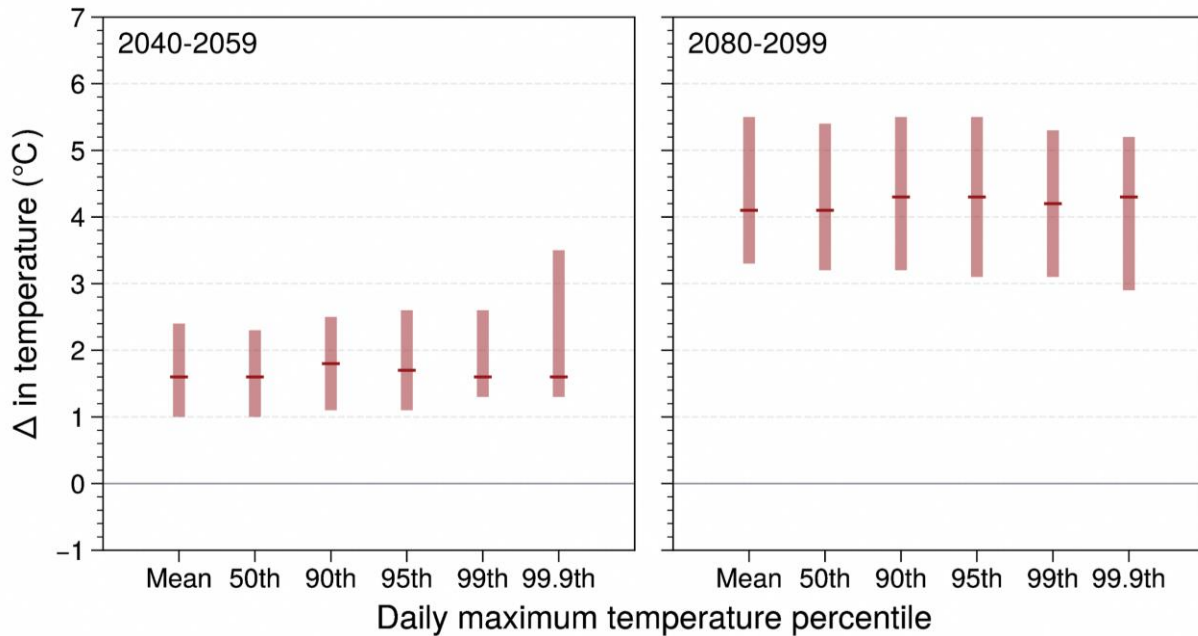
February – March



April – May



June – September



October – November

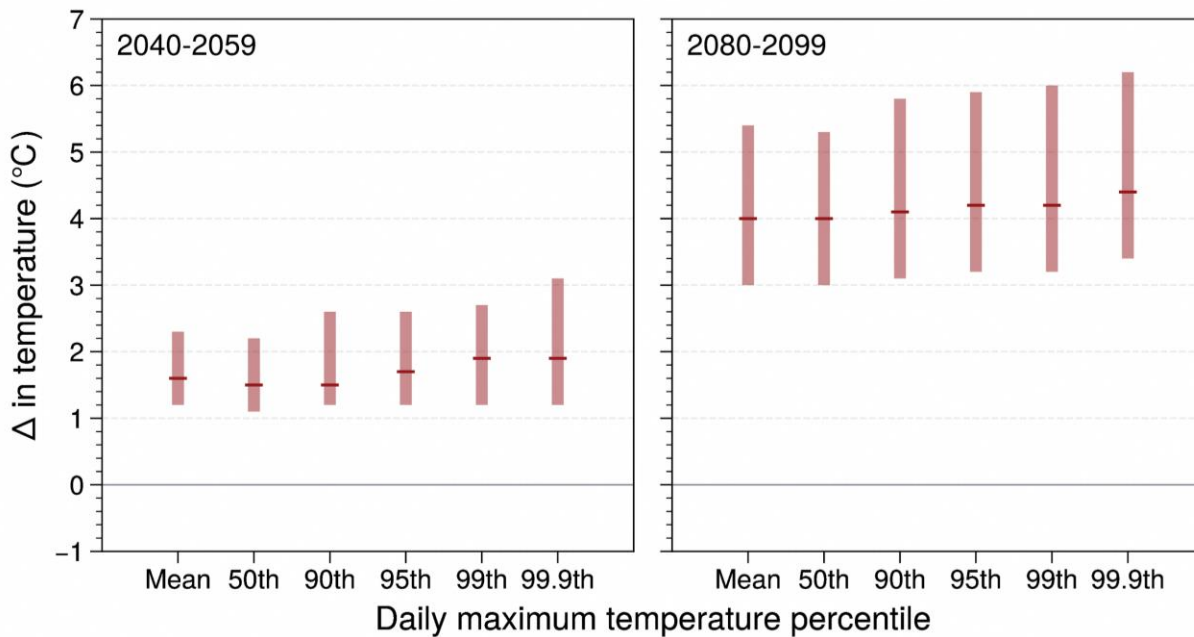


Figure A10.2: Range of changes in mean and extreme daily maximum temperature percentile amounts for various seasons (December-January, wet NE monsoon; February-March, dry NE monsoon; April-May, first intermonsoon; June-September; SW monsoon) from the 2-km SINGV-RCM simulations over Singapore. The median value in the range of percentage changes for each percentile is denoted by the dark red horizontal line. Each percentile uses the nearest corresponding daily maximum temperature value.

Figure A10.3 shows the projected changes of daily mean and extreme rainfall percentiles for Dec-Jan months over Singapore using 2 km and 8 km downscaled simulations in mid-century and

end century. In a 2km simulation, the mid-century's mean rainfall increased by 18% and extreme rainfall increased in the range of 15-35%. The mid-century mean rainfall from 8 km

simulation increased by 8% and extreme rainfall increased in the range of 3-20%. According to a 2 km simulation, the average rainfall increased by 10% at the end of the century, while extreme rainfall increased by 10% to 40%. In the end century from the 8 km simulations, the mean

rainfall increased by 3% and extreme rainfall varied in the range of -18 to 22%. During Dec-Jan months, the 2 km simulation had higher percentage increases in the mid and end century mean and extreme rainfall than the 8 km simulation.

December – January

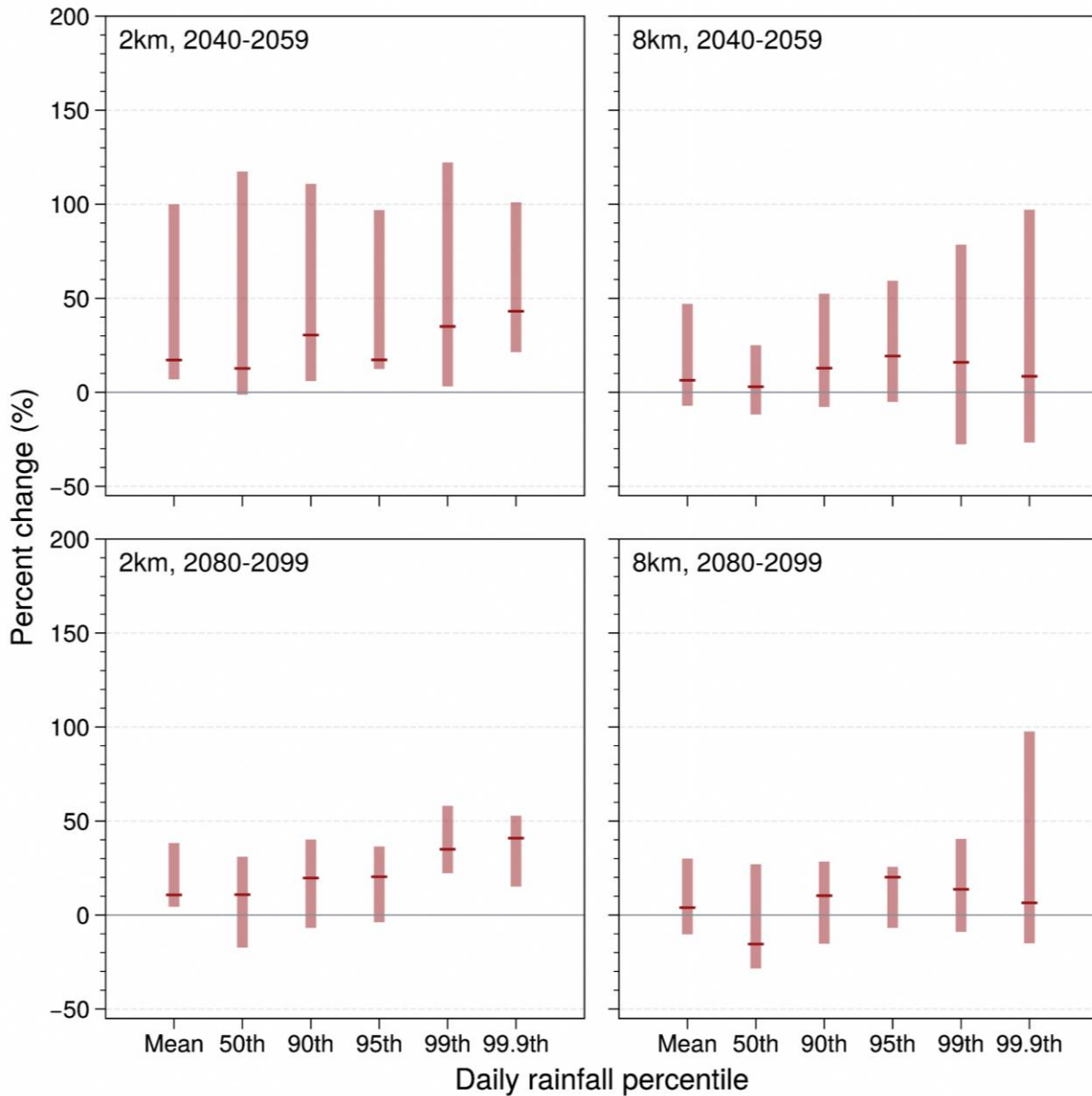


Fig A10.3: Changes in Singapore average daily rainfall amount during December - January (wet phase of NE monsoon) for the mid-century (2040-2059; top row) and end-century (2080-2099; bottom row) periods from SINGV-RCM downscaled simulations at 2-km (left) and 8-km (right). Shown are the percentage changes in the mean and at different percentiles (50th, 90th, 95th, 99th and 99.9th) under the SSP5-8.5 scenario. The mean and percentile values are derived only from wet days (rainfall \geq 1mm/day); each percentile uses the nearest corresponding daily rainfall value.

Figure A10.4 shows the projected changes of daily mean and extreme rainfall percentiles for Feb-Mar months over Singapore using 2km and 8km downscaled simulations in mid-century and end century. In the mid-century, the 2km simulation showed that mean rainfall increased by 25% and extreme rainfall increased in the range of 0-38%. In the 8 km simulation, the mid-century's mean rainfall increased by 25% and extreme rainfall increased in the range of 5-45%.

In the end century, the mean rainfall remained neutral and extreme rainfall varied in the range of -18 to 17% from 2 km simulation. The mean rainfall in the end century from the 8 km simulations remained unchanged whereas extreme rainfall varied in the range of -18 to 25%. The 2 km and 8 km simulation's mean and extreme rainfall projections often vary by almost the same amount for the months of February and March.

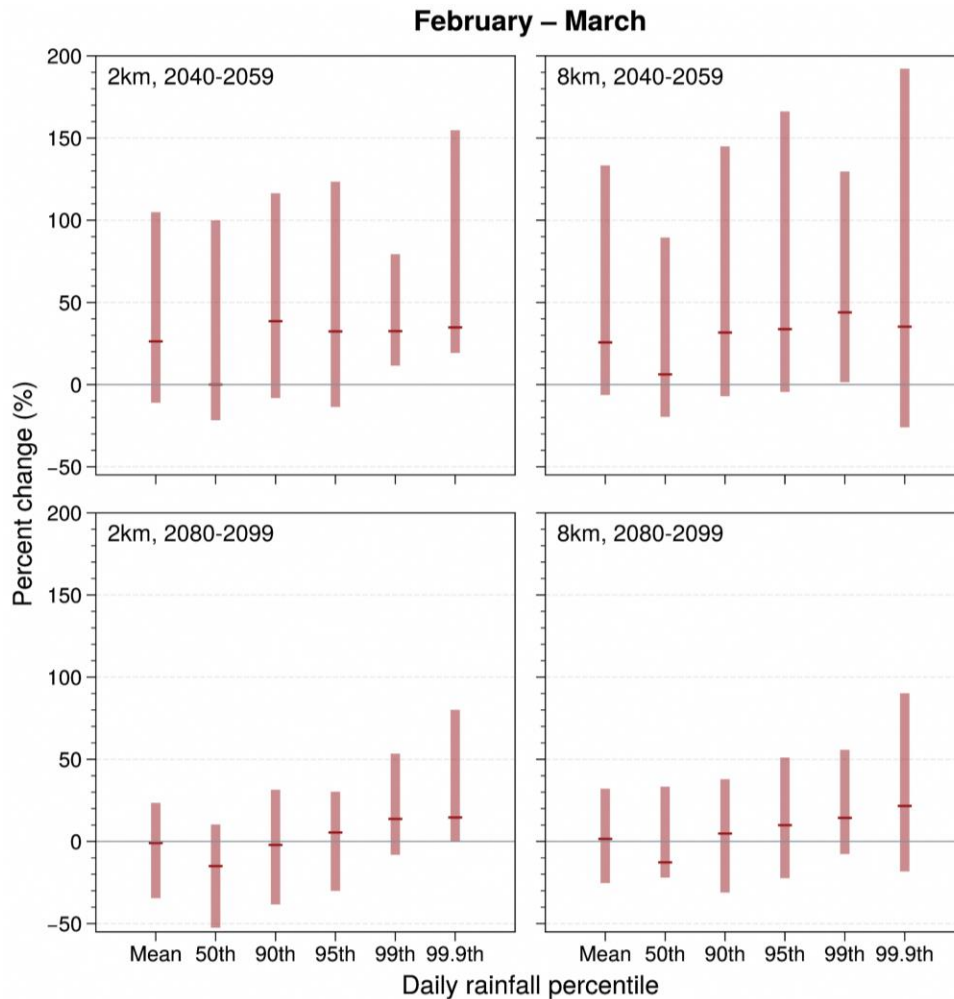


Figure A10.4: As in Figure A10.3 but for February - March (Dry phase of NE monsoon).

Figure A10.5 shows the projected changes of daily mean and extreme rainfall percentiles for Apr-May months over Singapore using 2 km and 8 km downscaled simulations in mid-century and end century. In a 2km simulation, the mid-century's mean rainfall increased by 5% and extreme rainfall increased in the range of 4-20%. The mid-century mean rainfall from 8 km

simulation increased by 5% and extreme rainfall increased in the range of 0-15%. According to a 2 km simulation, the average rainfall increased by 18% at the end of the century, while extreme rainfall increased by 0- 50%. In the end century from the 8 km simulations, the mean rainfall increased by 15% and extreme rainfall increased in the range of 0 to 25%. During Apr-May months,

the 2 km simulation had higher percentage increases in the mid and end century extreme rainfall than the 8 km simulation.

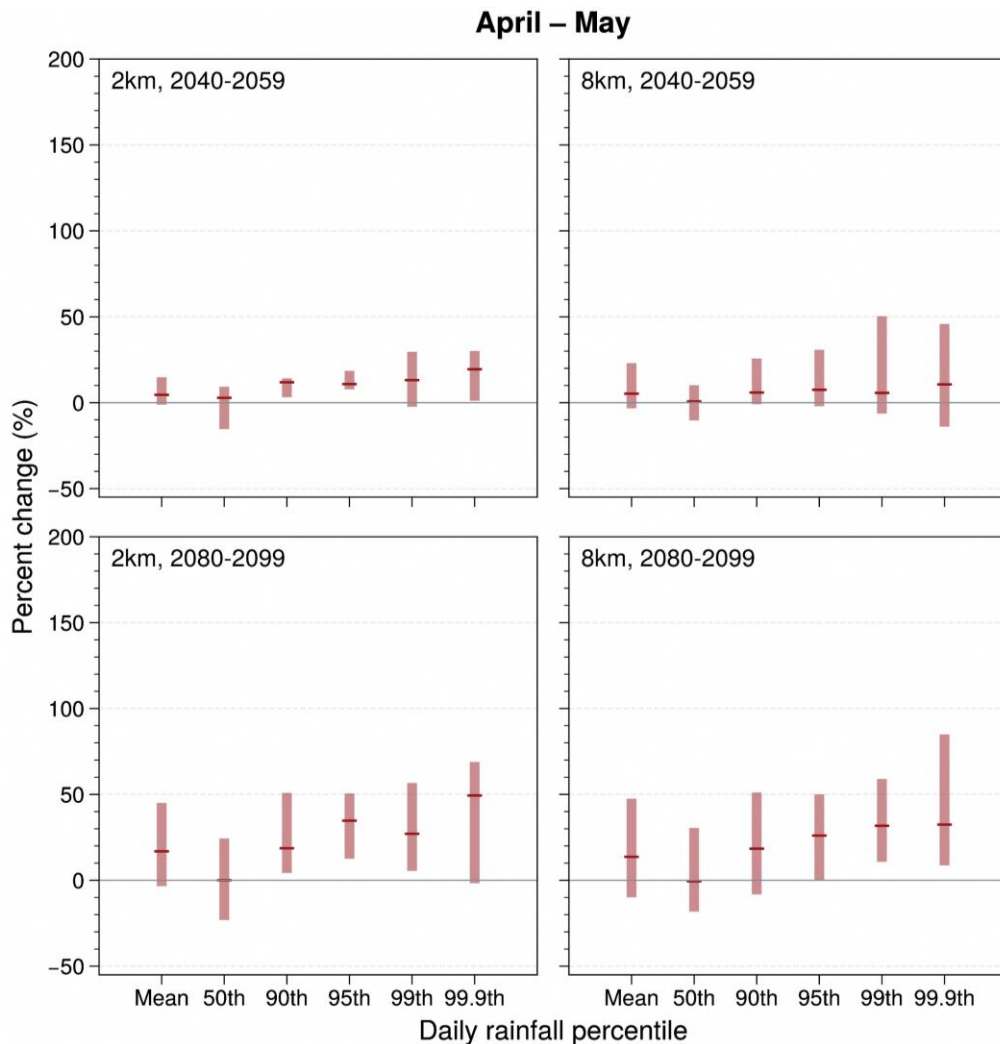


Figure A10.5: As in Figure A10.3 but for April-May

Figure A10.6 shows the projected changes of daily mean and extreme rainfall percentiles for Jun-Sep period over Singapore using 2km and 8km downscaled simulations in mid-century and end century. In the mid-century, the 2km simulation showed that mean rainfall increased by 2% and extreme rainfall varied in the range of -2 to 30%. In the 8 km simulation, the mid-century's mean rainfall increased by 1% and extreme

rainfall varied in the range of -2 to 15%. In the end century, the mean rainfall increased by 15% and extreme rainfall varied in the range of -2 to 25% from 2 km simulation. The mean rainfall in the end century from the 8 km simulations increased by 13% whereas extreme rainfall varied in the range of 0 to 20%. Similar to the Apr-May months, the 2 km simulation has higher percentage changes in the extreme rainfall than the 8 km simulation.

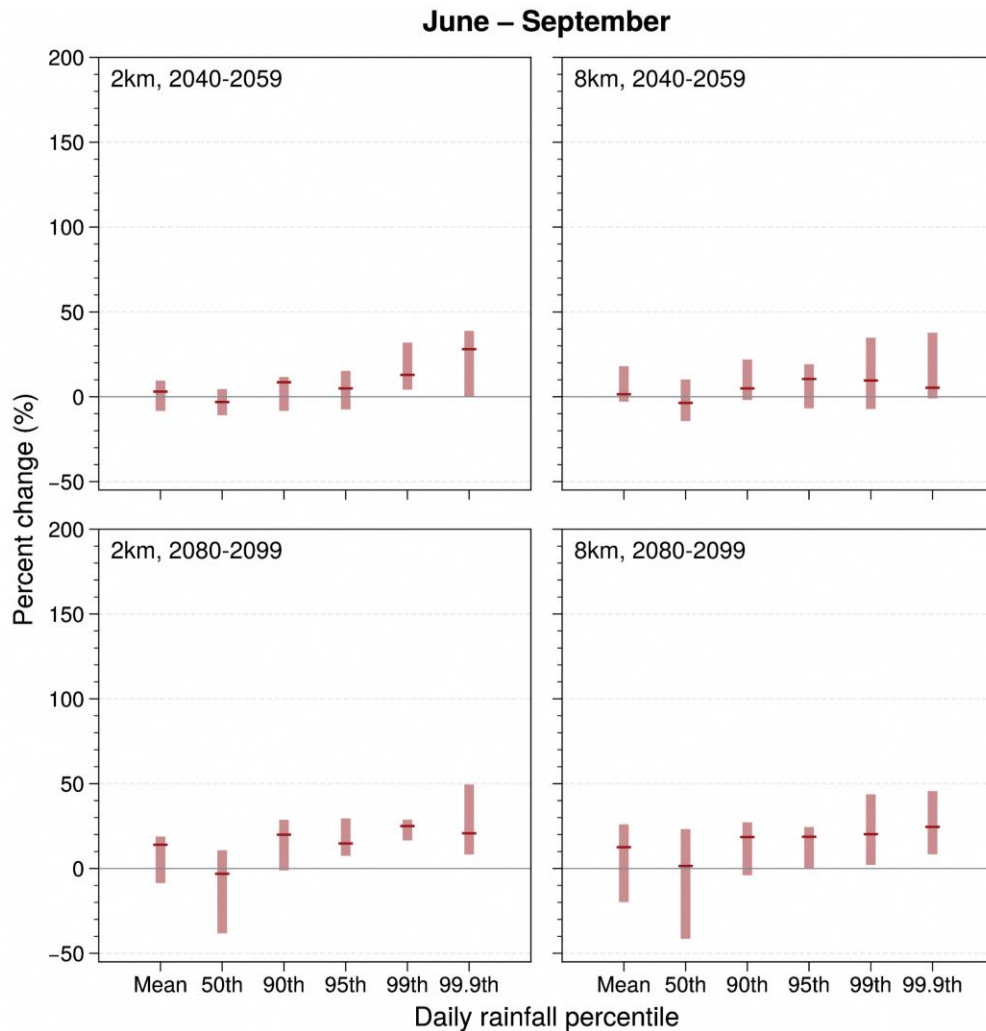


Figure A10.6: As in Figure A10.3 but for June - September (SW monsoon period).

Figure A10.7 shows the projected changes of daily mean and extreme rainfall percentiles for Oct-Nov months over Singapore using 2 km and 8 km downscaled simulations in mid-century and end century. In a 2km simulation, the mid-century's mean rainfall increased by 10% and extreme rainfall increased in the range of 5-25%. The mid-century mean rainfall from 8 km simulation increased by 17% and extreme rainfall increased in the range of 15-25%. According to a

2 km simulation, the average rainfall increased by 15% at the end of the century, while extreme rainfall increased by 5- 60%. In the end century from the 8 km simulations, the mean rainfall increased by 22% and extreme rainfall increased in the range of 10 to 55%. In contrast to the other months, in Oct-Nov months the 8 km simulation had higher percentage changes in the mean and extreme rainfall.

October – November

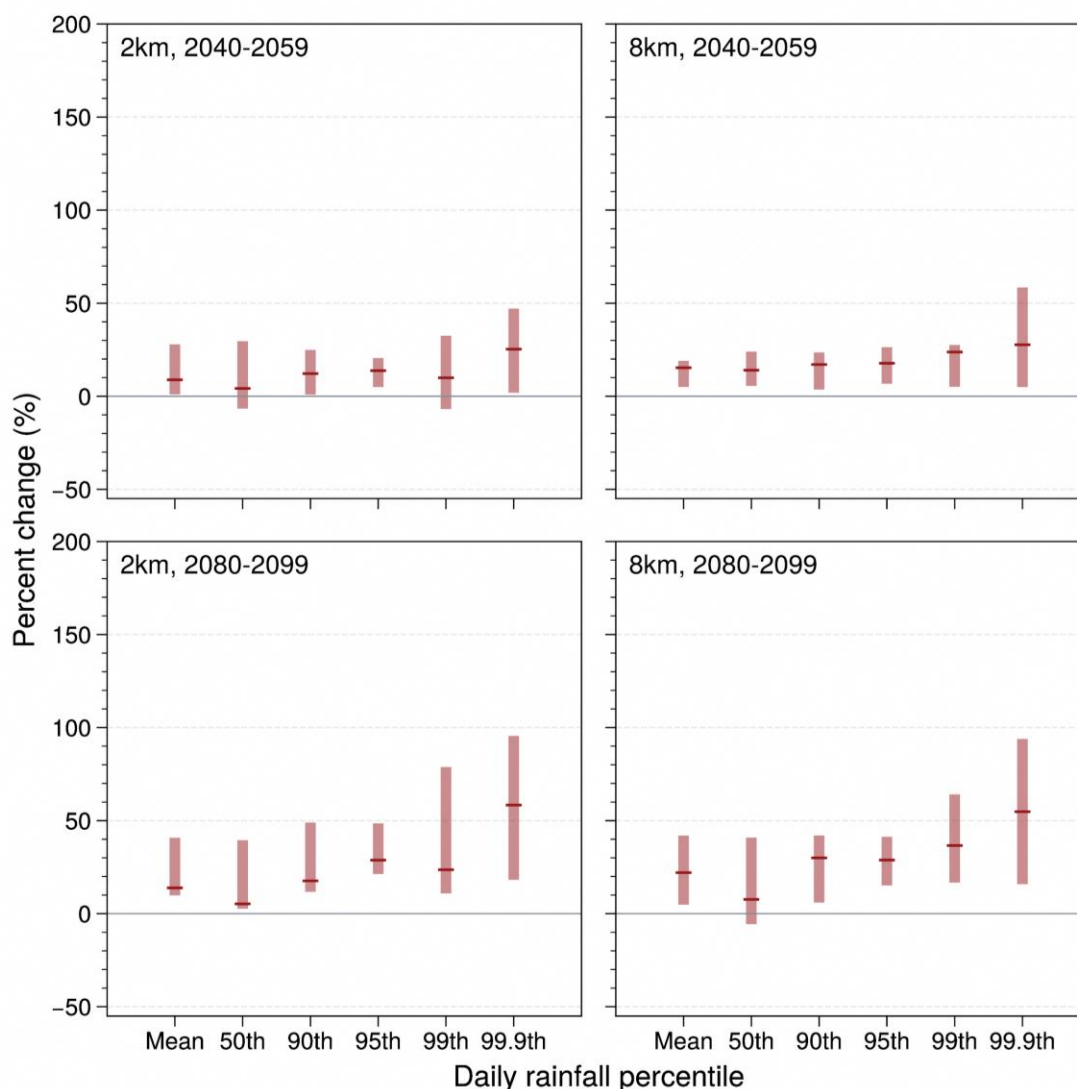


Figure A10.7: As in Figure A10.3 but for October-November (2nd intermonsoon)

Temperature

Figure A10.8 shows the projected changes of daily mean and extreme temperature percentiles for Dec-Jan months over Singapore using 2km and 8km downscaled simulations in mid-century and end century. In the mid-century, the 2km simulation showed that mean temperature is projected to increase by 1.3°C and extreme temperatures could increase in the range of 1.2°C to 1.7°C. In the 8 km simulations, in the mid-century the mean temperature is projected to

increase by 1.4°C and extreme temperature is projected to increase in the range of 1.4°C to 1.7°C. In the end century, for the 2 km simulation the mean temperature is projected to increase by 3.6°C and extreme temperature is projected to increase in the range of 3.6°C to 4.3°C. The mean temperature in the end century from the 8 km simulations is projected to increase by 3.4°C, whereas extreme temperature is projected to increase in the range of 3.4°C to 3.6°C. The mean and extreme temperature variations at the mid-century and end-of-century time frames vary only slightly across 2 km and 8 km simulations.

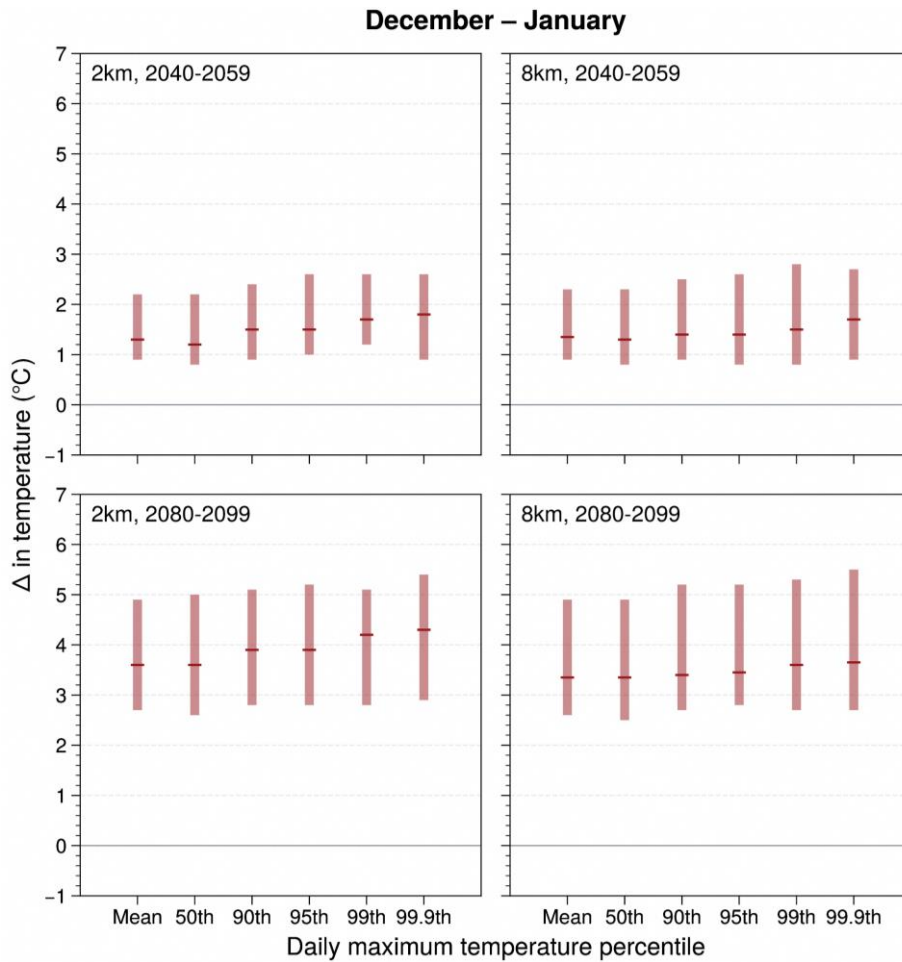


Figure A10.8: Changes in Singapore average daily maximum temperature during December - January (wet phase of NE monsoon) for the mid-century (2040-2059; top row) and end-century (2080-2099; bottom row) periods from SINGV-RCM downscaled simulations at 2-km (left) and 8-km (right). Shown are the percentage changes in the mean and at different percentiles (50th, 90th, 95th, 99th and 99.9th) under the SSP5-8.5 scenario. Each percentile uses the nearest corresponding daily maximum temperature value.

Figure A10.9 shows the projected changes of daily mean and extreme temperature percentiles for Feb-Mar months over Singapore using 2 km and 8 km downscaled simulations in mid-century and end century. In the 2km simulations, the mid-century mean temperature is projected to increase by 1.5°C and extreme temperature is projected to increase in the range of 1.4°C to 1.6°C. The mid-century mean temperature from 8 km simulations is projected to increase by 1.3°C and extreme

temperature is projected to increase in the range of 1.3°C to 1.6°C. Based on the 2 km simulations, the mean temperature is projected to increase by 3.5°C at the end of the century, while extreme temperature is projected to increase in the range of 3.5°C - 4.3°C. In the end century, from the 8 km simulations, the mean temperature is projected to increase by 3.4°C and extreme temperature is projected to increase in the range of 3.4°C to 3.8°C.

February – March

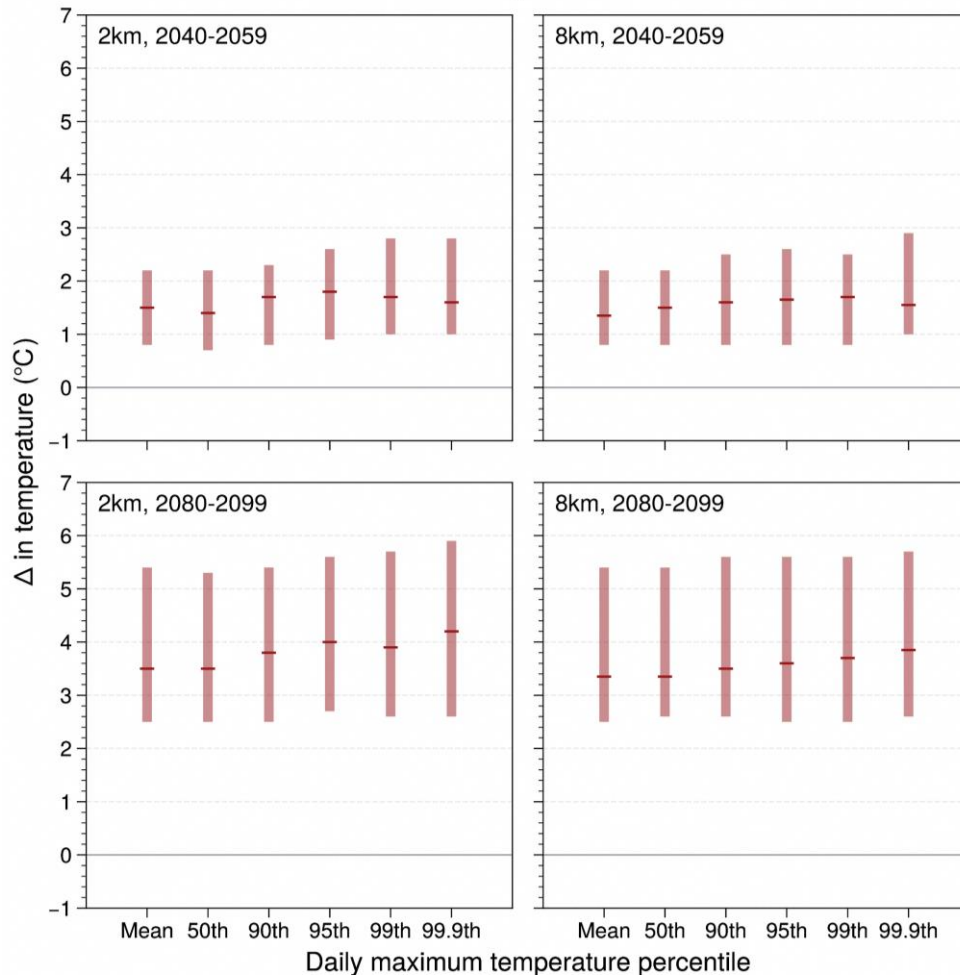


Figure A10.9: As in Figure A10.8 but for February - March (Dry phase of NE monsoon).

Figure A10.10 shows the projected changes of daily mean and extreme temperature percentiles for Apr-May months over Singapore using 2km and 8km downscaled simulations in mid-century and end century. In the mid-century, the 2km simulation showed that mean temperature is projected to increase by 1.3°C and extreme temperature is projected to increase in the range of 1.2°C to 1.7°C. In the 8 km simulation, the mid-century's mean temperature is projected to

increase by 1.4°C and extreme temperature is projected to increase in the range of 1.4°C to 1.7°C. In the end century, for the 2 km simulation the mean temperature is projected to increase by 3.6°C and extreme temperature is projected to increase in the range of 3.6°C to 4.3°C. The mean temperature in the end century from the 8 km simulations is projected to increase by 3.4°C, whereas extreme temperature is projected to increase in the range of 3.4°C to 3.6°C.

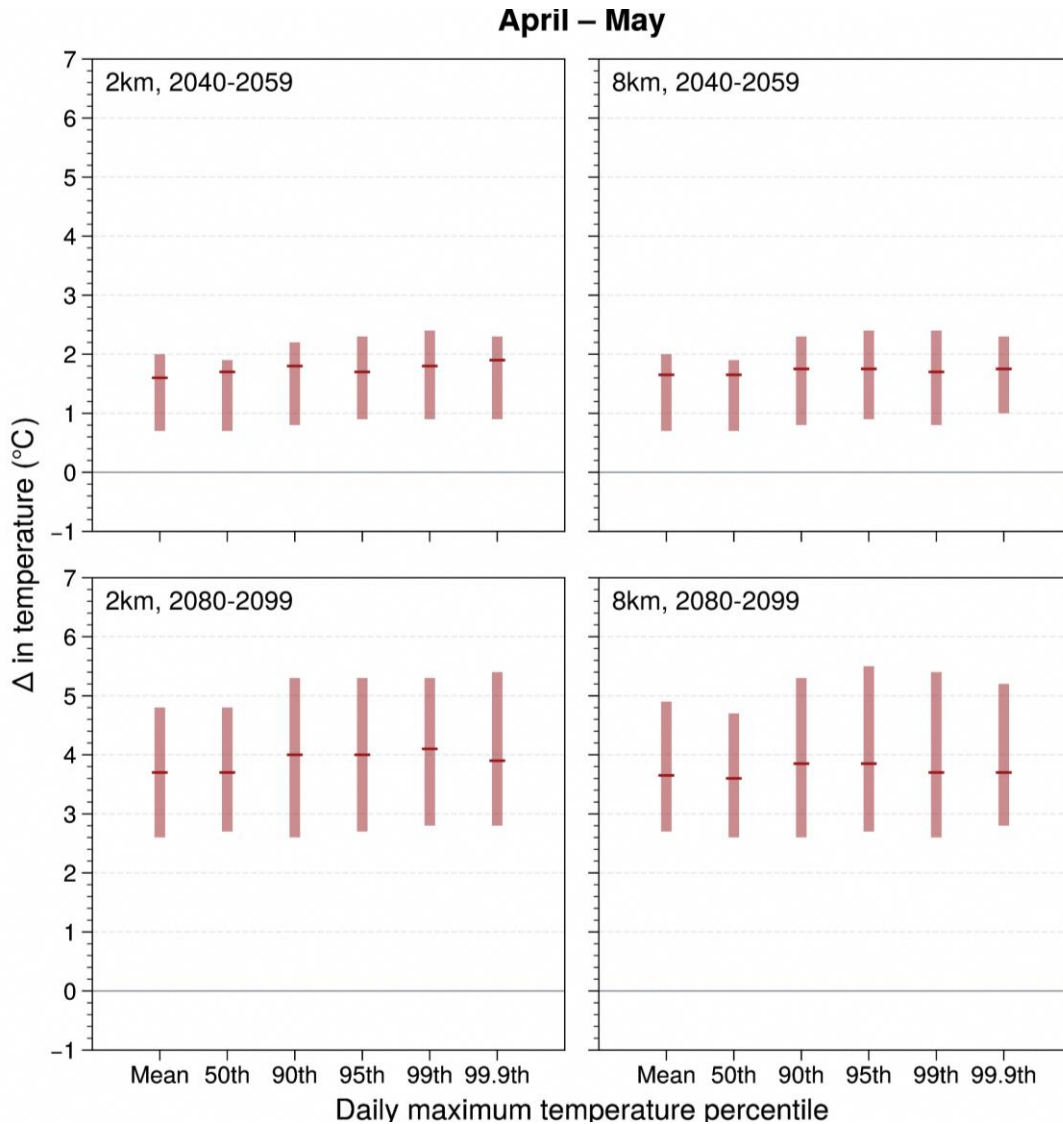


Figure A10.10: As in Figure 10.8 but for April-May

Figure A10.11 shows the projected changes in daily mean and extreme temperature percentiles for Jun-Sep period over Singapore using 2 km and 8 km downscaled simulations during mid-century and end century. Based on 2 km simulations, the mid-century's mean temperature is projected to increase by 1.6°C and extreme temperature is projected to increase in the range of 1.6°C to 1.8°C. The mid-century mean temperature, from 8 km simulations is projected to increase by 1.5°C

and extreme temperature is projected to increase in the range of 1.5°C to 1.6°C. Based on 2 km simulations, the mean temperature is projected to increase by 4.1°C at the end of the century, while extreme temperature is projected to increase in the range of 4.1°C - 4.4°C. In the end century, from the 8 km simulations, the mean temperature is projected to increase by 3.7°C and extreme temperature is projected to increase in the range of 3.7°C to 3.9°C.

June – September

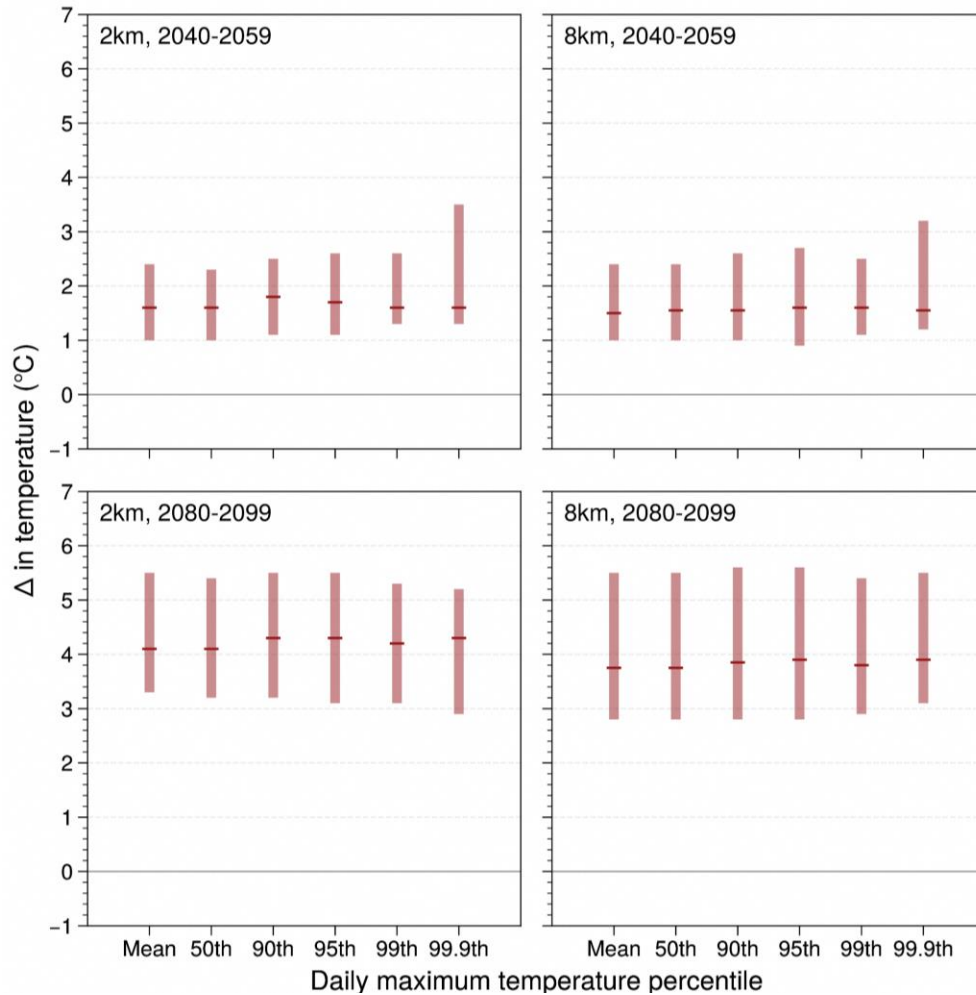


Figure A10.11: As in Figure A10.8 but for June - September (SW monsoon period).

Figure A10.12 shows the projected changes of daily mean and extreme temperature percentiles for Oct-Nov months over Singapore using 2km and 8km downscaled simulations in mid-century and end century. In the mid-century, the 2km simulation showed that mean temperature is projected to increase by 1.6°C and extreme temperature is projected to increase in the range of 1.5°C to 1.9°C. In the 8 km simulations, the mid-century's mean temperature is projected to increase by 1.3°C and extreme temperature is projected to increase in the range of 1.3°C to

1.7°C. In the end century, from the 2 km simulations the mean temperature is projected to increase by 4.0°C and extreme temperature is projected to increase in the range of 4.0°C to 4.5°C. The mean temperature in the end century from the 8 km simulations is projected to increase by 3.4°C, whereas extreme temperature is projected to increase in the range of 3.4°C to 4.1°C. Between 2 km and 8 km simulations, there are modest differences in the mean and extreme temperature changes at the mid-century and end-of-century.

October – November

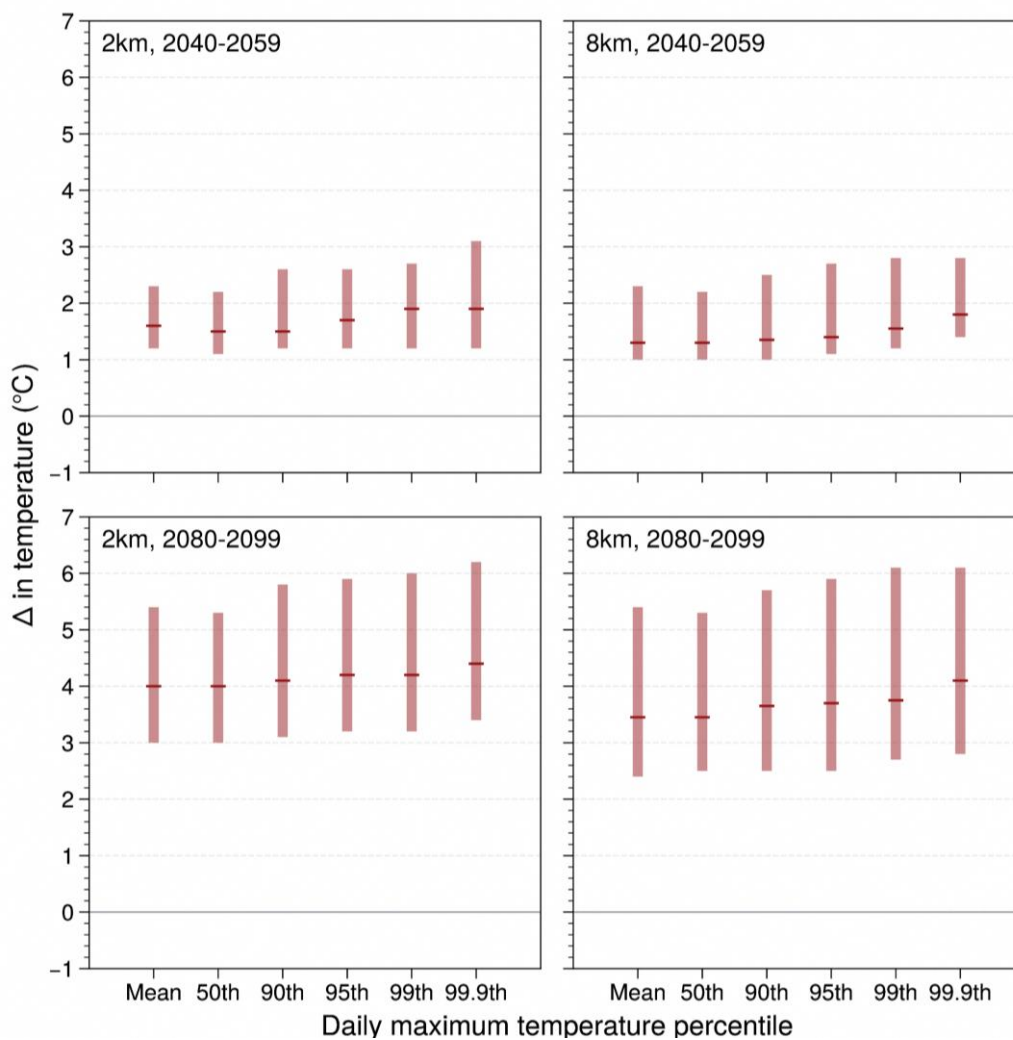


Figure A10.12: As in Figure A10.8 but for October–November (2nd intermonsoon)

Appendix B - Changes in winds over the WMC domain

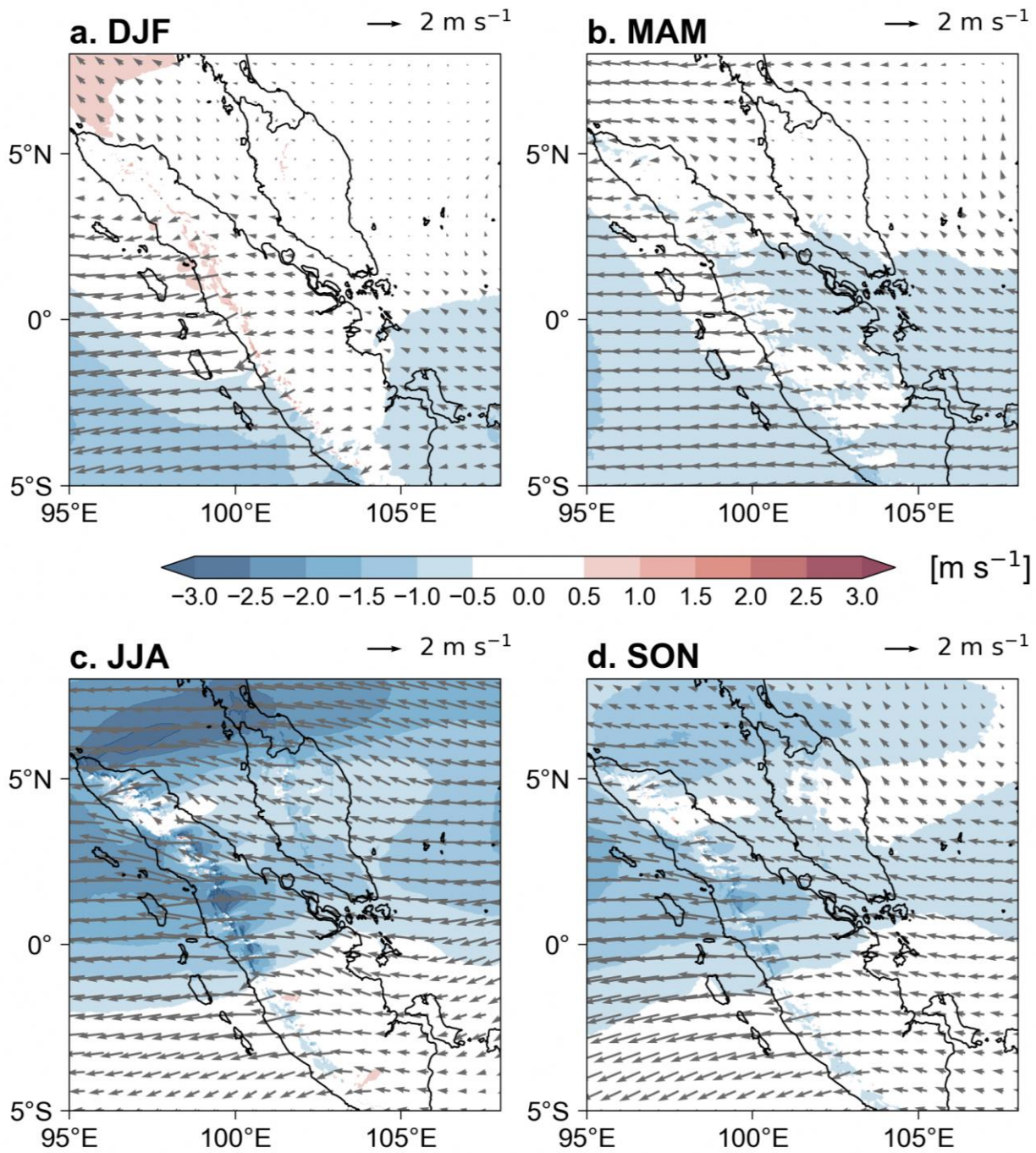


Figure B10.1: Changes in 850 hPa wind direction and climatological wind speeds (colors) in (a) DJF, (b) MAM, (c) JJA, (d) SON over Southeast Asia during 2080-2099 in SSP5-8.5 with respect to 1995-2014 in SINGV-MMM (containing five 2km model outputs).

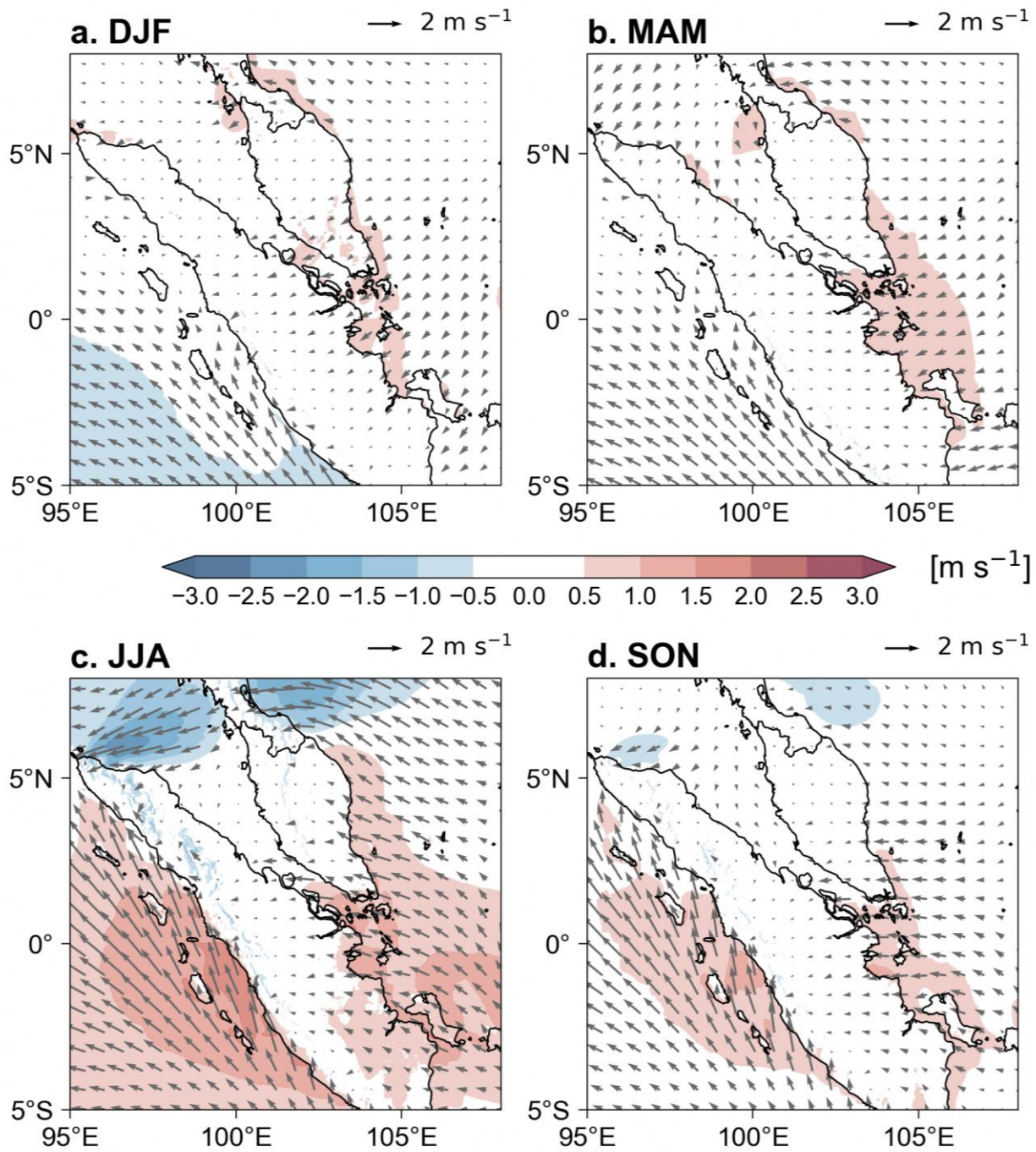


Figure B10.2: As in Figure B10.1 but for near-surface winds.

Appendix C – Changes in warm nights and very hot days

C10.1 How will the annual occurrence of warm nights change?

The frequency of occurrence of warm nights (daily minimum temperature equal to or exceeding 26.3

°C) is projected to increase in the future. Based on the observations record, Singapore has around 76 warm nights annually, and this number is projected to increase in the future, with warm nights becoming an everyday occurrence, by end-century, under the high emissions scenario. Projected changes for the mid- and end-century for all SSPs are shown in Table C10.1.

Table C10.1: Observed and projected number of warm nights annually, during mid- and end-century under the 3 SSP scenarios.

Scenario	Number of warm nights annually	
Observations	76 nights	
Future	Mid-Century	End-Century
SSP1-2.6	336 (317 to 352)	342 (312 to 361)
SSP2-4.5	347 (327 to 360)	362 (360 to 365)
SSP5-8.5	354 (335 to 364)	365 (365)

C10.2 How will the annual occurrence of very hot days change?

Very hot days are defined as days with daily maximum temperature exceeding 35 °C, based on the 99th percentile of daily maximum temperature. Historically, the average annual occurrence of very hot days are 21.4 days.

The frequency of occurrence of very hot days is projected to increase in the future. Based on the observations record, Singapore has around 21 very hot days annually, and this number is projected to increase in the future, with the worst case of almost every day being a very hot day by the end century under the high emissions scenario. Projected changes for the mid- and end-century for all SSPs are shown in Table C10.2.

Table C10.2: Observed and projected number of very hot days annually, during mid- and end-century under the three SSP scenarios.

Scenario	Number of very hot days annually	
Observed	21.4 days	
Future	Mid-Century	End-Century
SSP1-2.6	73 (47 to 93)	85 (41 to 125)
SSP2-4.5	95 (63 to 134)	173 (103 to 261)
SSP5-8.5	129 (76 to 189)	305 (252 to 351)